

A COMPUTATIONAL MODEL FOR ANEURYSM GROWTH

KHAIRUL FAEZI BIN MOHAMAD ALIAS @ AYIT

BACHELOR OF ENGINEERING
UNIVERSITI MALAYSIA PAHANG

2010

UNIVERSITI MALAYSIA PAHANG
FACULTY OF MECHANICAL ENGINEERING

I certify that the project entitled “A Computational Model for Aneurysm Growth” is written by Khairul Faezi Bin Mohamad Alias @ Ayit. I have examined the final copy of this project and in our opinion; it is fully adequate in terms of scope and quality for the award of the degree of Bachelor of Engineering. I herewith recommend that it be accepted in partial fulfillment of the requirements for the degree of Bachelor of Mechanical Engineering.

Mr. Mohd Fadzil Abdul Rahim

Examiner

Signature

UNIVERSITI MALAYSIA PAHANG

BORANG PENGESAHAN STATUS TESIS ♦

JUDUL: A COMPUTATIONAL MODEL FOR ANEURYSM GROWTH

SESI PENGAJIAN: 2010/2011

Saya, **KHAIRUL FAEZI BIN MOHAMAD ALIAS @ AYIT (881122-08-6459)**
(HURUF BESAR)

mengaku membenarkan tesis (Sarjana Muda / ~~Sarjana / Doktor Falsafah~~)* ini disimpan di perpustakaan dengan syarat-syarat kegunaan seperti berikut:

1. Tesis ini adalah hakmilik Universiti Malaysia Pahang (UMP).
2. Perpustakaan dibenarkan membuat salinan untuk tujuan pengajian sahaja.
3. Perpustakaan dibenarkan membuat salinan tesis ini sebagai bahan pertukaran antara institusi pengajian tinggi.
4. **Sila tandakan (√)

SULIT

(Mengandungi maklumat yang berdarjah keselamatan atau kepentingan Malaysia seperti yang termaktub di dalam AKTA RAHSIA RASMI 1972)

TERHAD

(Mengandungi maklumat TERHAD yang telah ditentukan oleh organisasi / badan di mana penyelidikan dijalankan)

TIDAK TERHAD

Disahkan oleh:

(TANDATANGAN PENULIS)

(TANDATANGAN PENYELIA)

Alamat Tetap:

**NO. 285, LORONG KANAN,
JALAN PADANG TEMBAK,
36000 TELUK INTAN, PERAK**

MOHD AKRAMIN BIN MOHD ROMLAY
(Nama Penyelia)

Tarikh: **6 DISEMBER 2010**

Tarikh: **6 DISEMBER 2010**

CATATAN: * Potong yang tidak berkenaan.

** Jika tesis ini SULIT atau TERHAD, sila lampirkan surat daripada pihak berkuasa/organisasi berkenaan dengan menyatakan sekali tempoh tesis ini perlu dikelaskan sebagai SULIT atau TERHAD.

♦ Tesis dimaksudkan sebagai tesis bagi Ijazah Doktor Falsafah dan Sarjana secara Penyelidikan, atau disertasi bagi pengajian secara kerja kursus dan penyelidikan, atau Laporan Projek Sarjana Muda (PSM).

A COMPUTATIONAL MODEL FOR ANEURYSM GROWTH

KHAIRUL FAEZI BIN MOHAMAD ALIAS @ AYIT

Report submitted in partial fulfillment of the requirements for the award of the degree of
Bachelor of Mechanical Engineering

Faculty of Mechanical Engineering
UNIVERSITI MALAYSIA PAHANG

DECEMBER 2010

SUPERVISOR'S DECLARATION

I hereby declare that I have checked this project and in my opinion, this project is adequate in terms of scope and quality for the award of the degree of Bachelor of Mechanical Engineering.

Signature

Name of Supervisor : MOHD AKRAMIN BIN MOHD ROMLAY

Position : LECTURER

Date : 6 DECEMBER 2010

STUDENT'S DECLARATION

I hereby declare that the work in this project is my own except for quotations and summaries which have been duly acknowledged. This project has not been accepted for any degree and is not concurrently submitted for award of other degree.

Signature

Name : KHAIRUL FAEZI BIN MOHAMAD ALIAS @ AYIT

Id. Number : MA07066

Date : 6 DECEMBER 2010

Dedicated to my beloved mother, Mrs. Kamariah Bt Osman and my family members that have supported me throughout this project and as well as my supervisor.

ACKNOWLEDGEMENTS

I am grateful and would like to express my sincere gratitude to my supervisor Mr. Mohd Akramin b. Mohd Romlay for his germinal ideas, invaluable guidance, continuous encouragement and constant support in making this research possible. He has always impressed me with his outstanding professional conduct, his strong conviction for science, and his belief that a bachelor program is only a start of a life-long learning experience. I appreciate his consistent support from the first day I applied to graduate program to these concluding moments. I am truly grateful for his progressive vision about my training in science, his tolerance of my naive mistakes, and his commitment to my future career. I also sincerely thanks for the time spent proofreading and correcting my many mistakes.

My sincere thanks go to all my lab mates and members of the staff of the Mechanical Engineering Department, UMP, who helped me in many ways and made my stay at UMP pleasant and unforgettable.

I acknowledge my sincere indebtedness and gratitude to my mother Kamariah Bt. Osman for her love, dream and sacrifice throughout my life. I acknowledge the sincerity of my family members, who consistently encouraged me to carry on my higher studies in Malaysia. I cannot find the appropriate words that could properly describe my appreciation for their devotion, support and faith in my ability to attain my goals. Special thanks should be given to my committee members. I would like to acknowledge their comments and suggestions, which was crucial for the successful completion of this study.

ABSTRACT

The aneurysm is the abnormal bulging of a portion of an artery due weakness in the cerebral. This occurs when the mechanical behaviour exceeds the strength of the tissue. Investigation on the changes of flow phenomena and the mechanical behaviour in cerebral aneurysm had been studied. This thesis was focus on the computational model for cerebral aneurysm growth. The main objectives of this project are to investigate the important role of wall shear stress in initiation, growth and rupture of aneurysm and also the wall deformation due to the blood flow. The simulation had been done by using different geometry of aneurysms and analyzed in the MSC Patran and MSC Dytran software. In this analysis, the size of geometry diameter and thickness were varied in order to analyze the Fluid Structure Interaction between the arterial structure and the blood flow. The geometry thickness that had been used in this analysis was 0.35 mm, 0.45 mm and 0.55 mm. After the analysis, the maximum displacement of the cerebral aneurysm wall was increased and wall shear stress was decreased by the increasing of diameter of the cerebral. The maximum displacements for different thickness are 0.005111 mm, 0.005094 mm and 0.005078 mm. The maximum wall shear stresses for different thickness are 0.9167 Pa, 1.1078 Pa and 1.1683 Pa. As the size of an aneurysm increases, there is a potential of rupture of aneurysm and this can result in severe hemorrhage or even worst, fatal event. To avoid an aneurysm rupture, research must be carry out to find the alternative to solve this problem which is more valuable to people that have been suffered because of aneurysms.

ABSTRAK

Aneurisme merupakan kejadian salur darah dibahagian kepala yang mengalami keadaan bengkak. Perkara ini berlaku apabila keadaan mekanikal telah melebihi keadaan asal pada salur darah tersebut. Kajian ini telah menfokuskan kepada keadaan mekanikal pada salur darah. Tesis ini berkenaan dengan analisis secara simulasi ke atas pembentukan aneurisme di tengah otak. Objektif utama projek ini dilaksanakan adalah untuk mengkaji kepentingan tekanan pada dinding aneurisme semasa permulaan, pengembangan dan perpecahan aneurisme serta hubungan antara anjakan dinding aneurisme dengan darah yang mengalir. Simulasi dilakukan ke atas geometri arteri yang berbeza-beza menggunakan perisian MSC Patran dan perisian MSC Dytran. Dalam analisis ini, saiz diameter dan ketebalan arteri yang digunakan adalah berbeza-beza bagi menganalisis hubungan antara struktur salur darah dan darah yang mengalir. Ketebalan geometri yang digunakan dalam analisis ini adalah 0.35 mm, 0.45 mm dan 0.55 mm. Selepas analisis dijalankan, didapati anjakan yang paling tinggi akan bertambah dan tekanan pada dinding aneurisme akan berkurang terhadap peningkatan saiz diameter aneurisme. Anjakan yang paling tinggi bagi ketebalan yang berbeza-beza adalah 0.005111 mm, 0.005094 mm dan 0.005078 mm. Tekanan yang paling tinggi pada dinding aneurisme bagi ketebalan yang berbeza-beza adalah 0.9167 Pa, 1.1078 Pa dan 1.1683 Pa. Apabila saiz aneurisme meningkat, terdapat potensi untuk aneurisme pecah dan boleh menyebabkan pendarahan atau lebih teruk, iaitu kematian. Bagi mengelakkan perpecahan aneurisme, kajian hendaklah dijalankan untuk mencari alternatif bagi menyelesaikan masalah ini yang begitu penting kepada orang menderita akibat aneurisme.

TABLE OF CONTENTS

		Page
EXAMINER’S DECLARATION		ii
SUPERVISOR’S DECLARATION		iii
STUDENT’S DECLARATION		iv
ACKNOWLEDGEMENTS		v
ABSTRACT		vi
ABSTRAK		vii
TABLE OF CONTENTS		viii
LIST OF TABLES		xi
LIST OF FIGURES		xii
LIST OF SYMBOLS		xv
LIST OF ABBREVIATIONS		xvi
CHAPTER 1 INTRODUCTION		
1.1	Introduction	1
1.2	Problem Statement	3
1.3	Significant of Study	3
1.4	Projects Objectives	3
1.5	Projects Scopes	4
CHAPTER 2 LITERATURE REVIEW		
2.1	Introduction of Cerebral Aneurysm	5
2.2	History of Aneurysms	6
2.3	Symptoms and effects of Aneurysms	7
	2.3.1 Aortic Dissection	7
	2.3.2 Blood Clots	8
	2.3.3 Rupture, Bleeding and Vasospasm	8
	2.3.4 Hyponatremia	8
	2.3.5 Hydrocephalus	9
2.4	Engineering Parameters	9

2.5	Previous Experimental Study	10
	2.5.1 Experimental Study of Cerebral Aneurysm as model	10
	2.5.2 Experimental Study of Cerebral Aneurysm in rats	11
2.6	Previous Numerical Study	11
	2.6.1 Numerical Study of Hemodynamic and Wall Remodelling	12
	2.6.2 Numerical Study on Fluid-Structure Interaction Modelling	16
2.7	Conclusions	19

CHAPTER 3 METHODOLOGY

3.1	Introduction	20
3.2	Software	23
	3.2.1 SolidWork software	23
	3.2.2 MSC Patran software	23
	3.2.3 MSC Dytran software	24
3.3	Structural Analysis	25
	3.3.1 Geometry of Cerebral Aneurysm	25
	3.3.2 Arterial Structure	25
	3.3.3 Finite Element Analysis (FEA)	27
	3.3.4 Material Model	28
3.4	Fluid Flow	29
	3.4.1 Flow in Artery	29
	3.4.2 Laminar Flow in Artery	30
	3.4.3 Newtonian and Non-Newtonian Fluids	30
	3.4.4 Navier-Stokes Equation for Incompressible Flow	31
	3.4.5 Computational Fluid Dynamics (CFD)	32
3.5	Boundary Conditions	32
	3.5.1 Wall Boundary Conditions	32
	3.5.1 Inflow/Outflow Boundary Conditions	33
3.6	Fluid Structure Interaction	34
3.7	Modelling of the Artery	35
3.8	Conclusions	36

CHAPTER 4 RESULTS AND DISCUSSION

4.1	Introduction	37
4.2	Numerical Simulation Modelling	37

4.3	Material Properties	39
4.4	Arterial and Aneurysm Wall Deformation	40
4.5	Wall Shear Stress	44
4.6	Interaction between the Blood Flow and Wall Shear Stress	47
4.7	Conclusions	49

CHAPTER 5 CONCLUSION AND RECOMMENDATIONS

5.1	Introduction	50
5.2	Conclusions	50
5.3	Limitation	51
5.4	Recommendations	51

REFERENCES	52
-------------------	----

APPENDIX A	55
-------------------	----

APPENDIX B	69
-------------------	----

LIST OF TABLES

Table No.	Title	Page
2.1	Independent Parameters	9
2.2	Dependent Parameters	9
2.3	Dimensionless Parameters	10
2.4	Parameters used in the simulation	13
2.5	Parameters used in the simulation	17
3.1	Parameters used in the simulation	29
4.1	Material Properties used in the simulation	40
4.2	Result of the simulation	41
4.3	Maximum Wall Shear Stress for Cerebral Aneurysm	46

LIST OF FIGURES

Figure No.	Title	Page
2.1	Flow and Stress Boundary Conditions and resulting geometry after the internal stress pre-evaluation step	13
2.2	Wall Shear Stress and Streamline comparison for the corresponding geometries at the time instances $t = 6$ and $t = 6a$	15
2.3	Aneurysm models based on CT images	17
2.4	Spatial mean velocity (a) and pressure (b) waveforms	18
3.1	The Flow Diagram of the Project	21
3.2	The Flow Diagram of the Analysis	22
3.3	Definition of aspect ratio, $AR = h/d_n$ (h and d_n are height and neck width of the aneurysm)	26
3.4	3D artery for 0.55 mm thickness	35
3.5	3D artery for 0.45 mm thickness	35
3.6	3D artery for 0.35 mm thickness	36
4.1	The design of 3D artery in SolidWorks	38
4.2	The artery design after the meshing process	39
4.3	The euler design after the meshing process	39
4.4	The flow in the cerebral aneurysm for thickness 0.35 mm	41
4.5	Maximum displacement of cerebral aneurysm thickness 0.35 mm	42
4.6	Graph of the maximum displacement and maximum velocity against inner diameter	43
4.7	Graph of the maximum displacement and maximum velocity against thickness	43
4.8	The inlet velocity waveforms	45
4.9	The outlet pressure waveforms	45
4.10	Wall shear stress of cerebral aneurysm thickness 0.35 mm	46

4.11	The graph of maximum wall shear stress against inner diameter	47
4.12	The graph of maximum wall shear stress against thickness	47
4.13	Graph of the maximum pressure and maximum velocity against maximum displacement	48
6.1	Open new database	55
6.2	Create group for artery	56
6.3	Import Parasolid xmt file	56
6.4	Create the eulerian region	57
6.5	Create local coordinate system	57
6.6	Post artery	58
6.7	Create finite element mesh for artery	58
6.8	Elements equivalence	59
6.9	Create finite element for eulerian solid	59
6.10	Create material for artery	60
6.11	Create material for eulerian solid	60
6.12	Create properties for artery	61
6.13	Create properties for eulerian solid	61
6.14	Create displacement nodal	62
6.15	Create planar rigid wall	62
6.16	Initial condition euler for shape	63
6.17	Initial condition euler for initial value	63
6.18	Create region definition	64
6.19	Create flow	64
6.20	Create general coupling	65
6.21	Analysis in patran	65

6.22	Output request	66
6.23	Analysis in Dytran software	66
6.24	Read archive file	67
6.25	Insight	68
6.26	Result	68
6.27	Final Year Project (FYP) I	69
6.28	Final Year Project (FYP) II	70

LIST OF SYMBOLS

E	Modulus of elasticity
ν	Poisson's ratio
ρ	Density
μ	Dynamic viscosity
\dot{v}	Flow rate

LIST OF ABBREVIATIONS

AR	Artery Ratio
BCs	Boundary Conditions
CFD	Computational Fluid Dynamics
FEA	Finite Element Analysis
FSI	Fluid Structure Interaction
GUI	Graphical User Interface
MSC	MacNeal-Schwendler Corporation

CHAPTER 1

INTRODUCTION

1.1 PROJECT BACKGROUND

Aneurysms can be described by their shape. Traditionally, they are described as either ‘fusiform’ like a narrow cylinder or ‘saccular’ like a small sac, though alternatives have been proposed. An aneurysm occurs when there is an abnormal widening, bulging or ballooning in the wall of an artery. This happens because the blood vessel has weakened, or become thin, in that area and the bulge is filling with blood. The most common place an aneurysm develops is in the aorta, which is the body's main artery. It carries blood to other parts of the body from the heart. Rupture of cerebral aneurysm is the leading cause of subarachnoid hemorrhage (Van Gijn and Rinkel, 2001), one of the fatal diseases occurring in the human cerebral circulation.

There are four types of aneurysms that can develop. Two of those are in the aorta which is a thoracic aneurysm occurs in the thorax, or chest, while an abdominal aneurysm occurs in the section of the aorta that runs through the abdomen. Three out of four aortic aneurysms are abdominal. A cerebral aneurysm occurs in an artery of the brain. Cerebral aneurysm is linked to hemodynamics in the cerebral arterial network (Steiger, 1990). The fourth type of aneurysm is a peripheral aneurysm. This type can occur in any artery other than the aorta or brain. Common arteries where a peripheral aneurysm forms are the carotid artery in the neck, the popliteal artery in the thigh behind the knee, and the femoral artery in the groin.

In a true aneurysm the inner layers of a vessel have bulged outside the outer layer that normally confines them. The aneurysm is surrounded by these inner layers. A

false or pseudoaneurysm does not primarily involve such distortion of the vessel. It is a collection of blood leaking completely out of an artery or vein, but confined next to the vessel by the surrounding tissue. This blood-filled cavity will eventually either thrombose (clot) enough to seal the leak or it will rupture out of the tougher tissue enclosing it and flow freely between layers of other tissues or into looser tissues. Pseudoaneurysms can be caused by trauma that punctures the artery and are a known complication of percutaneous arterial procedures such as arteriography or of arterial grafting or of use of an artery for injection, such as by drug abusers unable to find a usable vein. Like true aneurysms they may be felt as an abnormal pulsatile mass on palpation.

Rupture and blood clotting are the risks involved with aneurysms. Rupture leads to drop in blood pressure, rapid heart rate, high cholesterol, and lightheadedness. The risk of death is high except for rupture in the extremities. Blood clots from popliteal arterial aneurysms can travel downstream and suffocate tissue. Only if the resulting pain and/or numbness are ignored over a significant period of time will such extreme results as amputation be needed. Blood clots should be treated with care as overpressure when trying to get rid of them can cause them to shift. Clotting in popliteal venous aneurysms is much more serious as the clot can embolise and travel to the heart or through the heart to the lungs. Risk factors for an aneurysm are diabetes, obesity, hypertension, tobacco use, alcoholism, and copper deficiency (Amstrong, 1997).

The occurrence and expansion of an aneurysm in a given segment of the arterial tree involves local hemodynamic factors and factors intrinsic to the arterial segment itself. The human aorta is a relatively low-resistance circuit for circulating blood. The lower extremities have higher arterial resistance, and the repeated trauma of a reflected arterial wave on the distal aorta may injure a weakened aortic wall and contribute to aneurysmal degeneration. Systemic hypertension compounds the injury, accelerates the expansion of known aneurysms, and may contribute to their formation. Detailed hemodynamics in aneurysms has been investigated experimentally (Tateshima et al., 2001) and computationally (Burlison et al. 1995; Foutrakis et al. 1999; Shojima et al. 2004; Cebra et al. 2005 and Torii et al. 2006) to understand better the mechanisms contributing to the aneurysm progression.

1.2 PROBLEM STATEMENT

An aneurysm occurs when a blood vessel or artery weakens and balloons out or widens. If someone has an aneurysm, the prevention of rupture is imperative. This is because many cases about the aneurysms are unable to detect the exact time for growth and rupture, which can lead to death. It is important to study about the aneurysms because can minimize the risk of aneurysm rupture.

To avoid an aneurysm rupture, research must be carry out to find the alternative to solve this problem which is more valuable to people that have been suffered because of aneurysms.

1.3 SIGNIFICANT OF STUDY

There are few significances of this study when objectives have been achieved as follow:

- (i) An aneurysm can be treated successfully if it can be found in time.
- (ii) Can identify all the types of aneurysms that can causes fatal if it grows and bursts.
- (iii) Provide information for the diagnosis and treatment of an unruptured aneurysm by elucidating the risk of rupture.

1.4 PROJECT OBJECTIVES

The objectives of this project include:

- (i) To investigate the important role of wall shear stress in initiation, growth and rupture of aneurysm.
- (ii) To investigate computationally on the wall deformation due to the blood flow.

1.5 PROJECT SCOPES

The scopes of this project are limited to:

- (i) Steady-state analysis for blood flow in the artery.
- (ii) Study on Finite Element Analysis (FEA) for the different size of artery structure.
- (iii) Interaction between fluid and structure done by using fluid-structure interaction (FSI) simulation.
- (iv) Effect of dome or geometry of the cerebral aneurysm to blood parameter.

CHAPTER 2

LITERATURE REVIEW

2.1 INTRODUCTION

A cerebral or brain aneurysm is a cerebrovascular disorder in which weakness in the wall of a cerebral artery or vein causes a localized dilation or ballooning of the blood vessel. Cerebral aneurysms arise at the bifurcation of blood vessels. They are primarily saccular in shape, but may have additional lobules or ‘nipples’ (Cebtral et al., 2005).

While cerebral aneurysm pathology and atherosclerosis are two of the most common lesions of the cardiovascular system, there is no clear understanding on their pathogenesis mechanisms. The occurrence of atherosclerotic plaques (Texon, 1990) and cerebral aneurysms (Resnick et al., 2003) in well-recognized arterial regions, along with their focal distribution in regions of curvature, bifurcation and branching of the vessels, suggests that fluid dynamics play a pivotal role in the localization of those lesions. Low wall stress and high oscillatory patterns of wall shear stress cause intimal wall thickening (Caro et al., 1969), while increased blood flow and a unidirectional flow environment are associated with vasodilation (Ziegler et al. 1997 and Ziegler et al. 1998).

Cerebral aneurysms involve both the anterior and posterior circulation. Rupture of a cerebral aneurysm causes subarachnoid hemorrhage with potentially severe neurologic complications (Schievink, 1997). Cerebral aneurysms are classified as saccular and non-saccular types, according to their shape and etiology. Typically, saccular aneurysms arise at a bifurcation or along a curve of the parent vessel.

Cerebral aneurysms are rarely formed in patients under 20 years of age and numbers peak between 60 and 80 years (Lindsay, 2007). Female gender increases the likelihood of an incidental aneurysm as does the presence of atherosclerosis. A family history of two or more affected first-degree relatives or a history of polycystic kidney disease increases the relative risk. Those patients who have undergone repair of a ruptured aneurysm have an increased tendency to form other aneurysms.

In this chapter, a little bit of historical background and a brief explanation on the symptoms and effects of aneurysms will be discussed. Then some discussion on cerebral aneurysms for different size of geometry, blood flow rate and the conditions of pressure and velocity will be explained. Besides, some discussion on the materials used as a model for cerebral aneurysms and together with the previous study in experimental and numerical about cerebral aneurysms will be discussed. Then it is followed by some of the result from previous study by researchers have been included as a references to this study. Finally, this chapter is ends by a conclusion from overall of this study.

2.2 HISTORY OF ANEURYSMS

In the fourteenth century B.C. the Egyptians, according to Sigerist (1951), treated aneurysms by magico-religious therapies, but the nature and site of occurrence of these lesions are not mentioned nor the term applied to them. Ruffer (1911) claimed that arterial degenerative diseases were prevalent amongst the Egyptians, so aneurysms of the aorta almost certainly occurred, though no reference to them has been found. Major (1954), quoting Ebbell, lists aneurysm and arteriovenous aneurysm amongst the diseases described in the Ebers Papyrus. The religious fears of the Egyptian embalmers seems to have been greater than their curiosity in the vast quantity of pathological material they handled, as Long (1933) suggests, for the diseases mentioned were primarily those discernible on external examination of the body.

From this time till the second century A.D. there appears to be no existing medical literature on aneurysms. It is probable that knowledge of these lesions was

mainly handed on by word of mouth. Galen (1628) is thus to be considered the first to define and describe the disease, recognizing the false variety and those arising spontaneously by dilatation. Adams (1846) states that Galen (1628) knew of and treated traumatic aneurysms following venesection in the cubital fossa. Considering the frequent use of venesection, and the fact that he is said by Castiglioni (1941) to have been physician to the gladiators, Galen (1628) probably saw traumatic aneurysms rather frequently. These lesions were easier to observe than the more deep-seated non-traumatic aneurysms which in modern medicine are more common.

Antyllos in the third century B.C, who according to Major (1954) appeared like a “comet on the surgical horizon”, made his greatest achievement by treating aneurysms in the second century A.D. Antyllos also recognized both the false and true varieties. Aetius in the sixth century, in a selected passage translated by Erichsen in 1884, described the clinical signs of aneurysms mentioning that they can occur in any part of the body, even in the head.

2.3 SYMPTOMS AND EFFECTS OF ANEURYSMS

A small brain aneurysm typically produces no symptoms, but a larger aneurysm can cause mydriasis (dilated pupil), double vision or blurry vision, ptosis (drooping eyelid), eye pain and facial paralysis (Amstrong, 1997). An aneurysm can also affect one of the largest and most important vessels of the heart called the aorta. The aorta extends from the heart to the chest region and down the stomach. Typically, aortic aneurysms are asymptomatic and inadvertently found through imaging. Both brain and aortic aneurysms have specific side effects.

2.3.1 Aortic Dissection

An aortic aneurysm can suddenly burst without warning. This is medically known as an aortic dissection. Symptoms of an aortic dissection include severe pain that radiates from the chest to the back. Prior to the pain, there may be a popping sound that is

indicative of tearing of the aorta. It can also cause stomach pain, a stroke and coldness or numbness of the legs or arms. This is a life-threatening side effect that requires immediate surgical repair.

2.3.2 Blood Clots

Aortic aneurysms increase the risk of blood clot formation. Usually, they can buildup near the weakened blood vessel, break off and move to the extremities and organs. This can lead to organ damage and peripheral ischemia, a condition in which the arms or legs do not receive enough blood flow.

2.3.3 Rupture, Bleeding and Vasospasm

Like an aortic aneurysm, a brain aneurysm can also rupture. The blood will leak into the brain and cause the following symptoms such as severe headache, nausea, vomiting, light sensitivity and blurry vision. It can also cause convulsions, unconsciousness and confusion. Patients are susceptible to re-bleeding episodes even after surgery. The leakage of blood can further damage the brain and cause the aforementioned symptoms. Also, the ruptured blood vessels in the brain can spasm (rapidly constrict and relax in succession). This can prevent adequate amounts of blood from reaching the brain, and can subsequently lead to a stroke. Symptoms of stroke include paralysis on one side of the body, slurred speech and difficulty seeing.

2.3.4 Hyponatremia

A brain aneurysm can cause hyponatremia (low blood sodium levels). This can lead to brain edema (swelling) and further brain destruction. Symptoms of hyponatremia include headache, convulsions, poor appetite, and loss of consciousness, coma and confusion. Typically, doctors will give patients intravenous (through the vein) fluids to increase patients' sodium levels.

2.3.5 Hydrocephalus

A brain aneurysm can also block the flow of cerebrospinal (clear fluid carrying nutrients and cells) fluid in the brain and spinal cord. This can lead to hydrocephalus, a condition in which excessive amounts of cerebrospinal fluid (CSF) cause increased intracranial (within the skull) pressure. Symptoms of hydrocephalus include headache and vomiting. A shunt can be placed into the brain to help drain the CSF.

2.4 ENGINEERING PARAMETERS FOR ANEURYSMS

The follow tables are a list of variables, their symbols, and the associative units commonly used in aneurysms expressions. All the equations present have the same quantity denoted by the symbols in the table and some of these parameters will be commonly used in this study.

Table 2.1: Independent parameters

Quantity	Symbol	Object	Units
Modulus of elasticity	σ	Scalar	Pa
Dynamic viscosity	μ	Scalar	kg/m.s
Density	ρ	Scalar	kg/m ³

Table 2.2: Dependent parameters

Quantity	Symbol	Object	Units
Pressure	P	Scalar	N/m ²
Velocity	V	Vector	m/s

Table 2.3: Dimensionless parameters

Parameter	Formula	Interpretation
Reynolds number	$Re = \frac{VD}{\nu}$ $= \rho VD/\mu$	Ratio of inertial forces to viscous forces in the fluid.
Poisson's ratio	$\nu = -\frac{\epsilon_{lat}}{\epsilon_{long}}$	Ratio of strains in the longitudinal or axial direction to the lateral or radial direction.

2.5 PREVIOUS EXPERIMENTAL STUDY OF ANEURYSMS

There are a lot of experiments have been carried out to study the aneurysms. Besides that, all these experiments are also conducted in order to investigate scientifically the behavior of different types of aneurysms under different conditions and properties. In this chapter, summary of previous experimental study of aneurysms and the results gathered from the study will be discussed.

2.5.1 Experimental Study of cerebral aneurysms as model for non-surgical treatment (Neurosci, 1994)

This article summarizes the results of our experimental studies on the pathogenesis of cerebral aneurysm. Experimentally induced aneurysms in rats and in monkeys resemble those of human cases both in location and in microscopic structure. By studying early changes of aneurysm development, it is proposed that degenerative changes in the intima caused by hemodynamic stress at vessel branches are the basis for aneurysm formation and aneurysms develop, at least partly, because of defective or decreased healing processes there.

By giving the experimental animals blood coagulation factor XIII, which is known to enhance wound healing, a significant amount of intimal proliferation occurred in and around aneurysms. Some aneurysms were completely obliterated. This fact may

indicate a possibility of non-surgical treatment of the disease in the future. Suggestive findings in human autopsy cases are also presented.

2.5.2 Experimental Study of cerebral aneurysms in rats: VII. Scanning electron microscope study (Neurol, 1981)

The luminal surfaces of experimentally induced cerebral aneurysms and the branching sites in the circle of Willis in rats were investigated by scanning electron microscopy. Gap formation at the junctions of the endothelial cells was one of the most obvious changes on the endothelial surface of the aneurysms. Many leukocytes were observed adhering to these gaps.

Regressive changes of endothelial cells, such as balloon like protrusions and craterlike depressions, were also found in the aneurysms. At the branching site, where cerebral aneurysms often develop, endothelial cells were disarranged, rounded, and varied in size. A deep groove was also found adjacent to the apex. The role of endothelial cells and leukocytes in the development of cerebral aneurysms is discussed.

2.6 PREVIOUS NUMERICAL STUDY OF ANEURYSMS

As discussed before in the previous chapter, there are lots of scientists and researchers conducted the experiments to investigate the behavior of aneurysms under certain conditions and properties. Actually, some of the previous experiments are not carried out experimentally only, but numerically too. By using numerical method, many different parameters can be investigated and study in order to achieved various result that cannot be conducted using experimental way. Besides, using this kind of method can save cost and time and the result still can be obtained with accuracy.

In this chapter, numerical investigation of aneurysms under different conditions and properties will be discussed.

2.6.1 Numerical Study of Hemodynamic and Wall Remodeling of a Growing Cerebral Aneurysm: A Computational Model (Chatziprodromou et al., 2007)

This hypothesis involves a combination of two parallel and interconnected mechanisms: according to the first mechanism, an endothelium-originating and wall shear stress-driven apoptotic behavior of smooth muscle cells, leading to loss of vascular tone is believed to be important to the aneurysm behavior. Vascular tone refers to the degree of constriction experienced by a blood vessel relative to its maximally dilated state. All resistance and capacitance vessels under basal conditions exhibit some degree of smooth muscle contraction that determines the diameter, and hence tone, of the vessel.

The second mechanism is connected to the arterial wall remodeling. Remodeling of the arterial wall under constant tension is a biomechanical process of rupture, degradation and reconstruction of the medial elastin and collagen fibers. In order to investigate these two mechanisms within a computationally tractable framework, we devise mechanical analogues that involve three-dimensional hemodynamic, yielding estimates of the wall shear stress and pressure fields and a quasi-steady approach for the apoptosis and remodeling of the wall.

These analogues are guided by experimental information for the connection of stimuli to responses at a cellular level, properly averaged over volumes or surfaces. The model predicts aneurysm growth and can attribute specific roles to the two mechanisms involved: the smooth muscle cell-related loss of tone is important to the initiation of aneurysm growth, but cannot account alone for the formation of fully grown sacks; the fiber-related remodeling is pivotal for the latter.

The model used in the simulation is shown in Figure 2.1 below. This initial geometry was used for a stress pre-evaluation step: Arteries at normal equilibrium conditions have residual stresses in the arterial walls, because of the blood flow and the pressure of the blood they contain. In order to model these stresses, performed an initial calculation, in a fully coupled fluid-structure interaction manner that was equivalent with

filling an unstressed (empty) artery with blood at physiological flow conditions. The resulting geometry of this initial computation with the calculated internal stresses was used as the base for all further calculations.

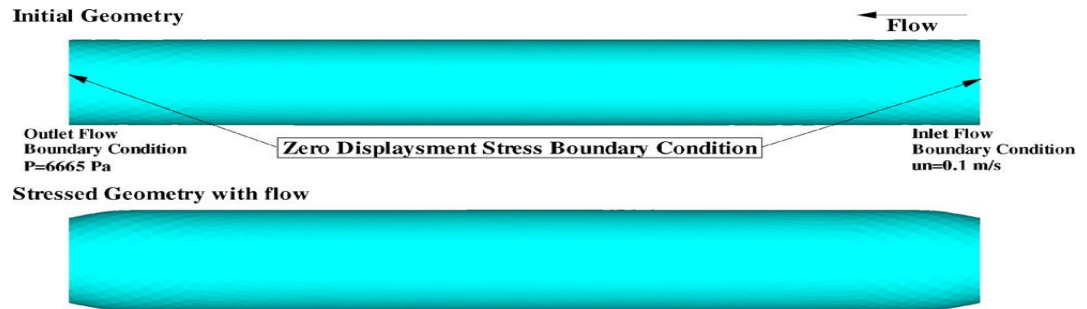


Figure 2.1: Flow and Stress Boundary Conditions and resulting geometry after the internal stress pre-evaluation step.

Source: I. Chatziprodromou et al., 2007

Table 2.4: Parameters used in the simulation

Quantity	Value	Units
Length of the tubular model, L	65	mm
Diameter of the carotid artery, D_o	6.5	mm
Thickness arterial wall, t	0.75	mm
Uniform Velocity inlet, V	0.1	m/s
Uniform Pressure outlet, P	6665	Pa
Modulus of elasticity, E	120000	Pa
Blood density, ρ	1069	kg/m ³
Blood dynamic viscosity, μ	0.0035	kg/m. s
Poisson's ratio, ν	0.4	
Reynolds number, Re	200	

Source: I. Chatziprodromou et al., 2007

After this initial step was completed, the general quasi-steady algorithm was employed to study the growth of an induced aneurysm in this pre-stressed arterial segment. The blood flow equations that were solved by the finite volume solver are the incompressible Navier–Stokes equations along with continuity, i.e. the conservation laws for momentum and mass for incompressible fluids. The conservation of mass can be expressed as

$$\frac{\partial u_i}{\partial x_i} = 0 \quad (2.1)$$

Conservation of momentum reads:

$$\rho \frac{\partial u_i}{\partial t} + \rho u_j \frac{\partial u_i}{\partial x_j} = -\frac{\partial p}{\partial x_i} + \frac{\partial \tau_{ij}}{\partial x_j} + S_{M_x} \quad (2.2)$$

The viscous stress components τ_{ij} read:

$$\tau_{ij} = 2\mu s_{ij} \text{ Where } s_{ij} = \frac{1}{2} \left(\frac{\partial u_i}{\partial x_j} + \frac{\partial u_j}{\partial x_i} \right) \quad (2.3)$$

For Newtonian flows with constant viscosity, μ .

In this simulation, I. Chatziprodromou and friends used (Gambit, FLUENT INC.) software to solve the equations for each parameter applied in this experiment. The results are shown in Figure 2.2.

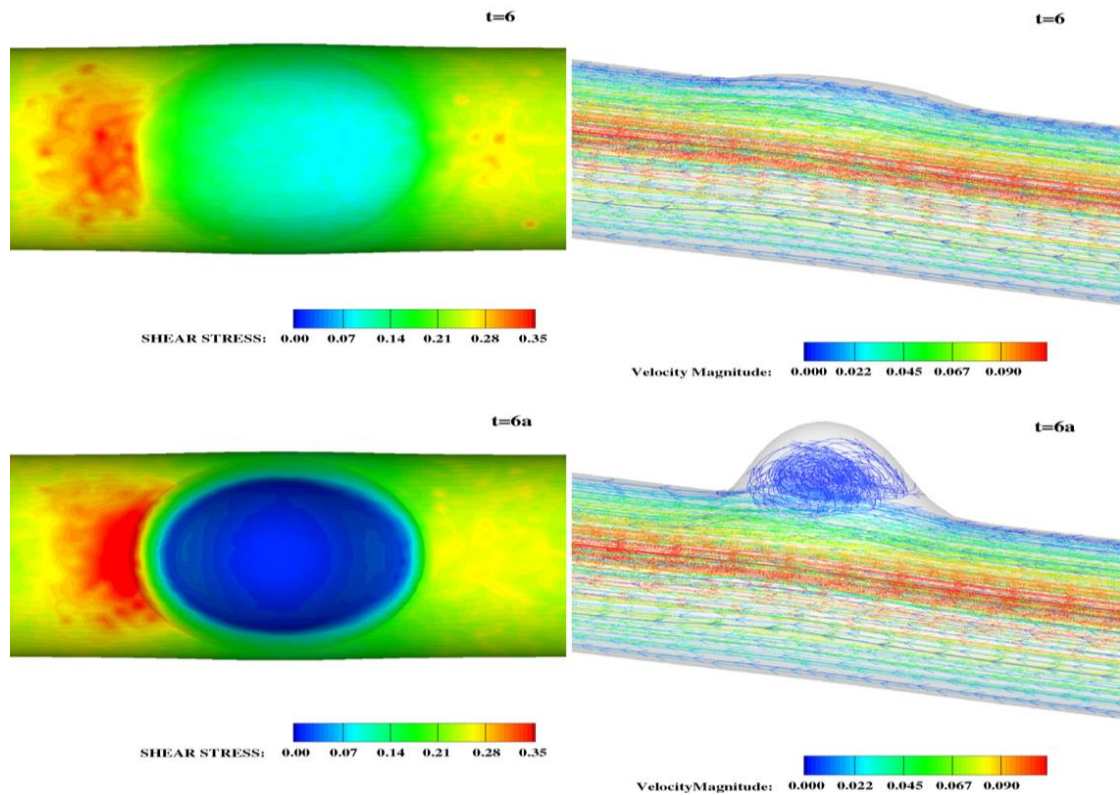


Figure 2.2: Wall Shear Stress and Streamline comparison for the corresponding geometries at the time instances $t = 6$ and $t = 6a$.

Source: I. Chatziprodromou et al., 2007

As conclusion from the data obtained, the model relies on certain simplifying assumptions: the bizonal approach, and the relation of smooth muscle cell tone loss and apoptosis with the WSS patterns are two of the most important ones. Moreover, for the purposes of the present study, we have limited the driving hemodynamic to steady state simulations.

On the other hand, correlating accurately detailed quantitative data of vasoactive agent overproduction with local wall shear stress patterns involves detailed in vitro or better yet in vivo experiments which, to the best of our knowledge, do not exist. With the above approximations, the model developed shows that the combination of two

individual mechanisms, often postulated in the literature as responsible for aneurysm growth, are indeed of importance to the process: Loss of vascular tone due to smooth muscle cell apoptosis and reconstitution of fibers after prolonged periods of excessive strain have been shown to contribute to the condition.

2.6.2 Numerical Study on Fluid–structure interaction modeling of blood flow and cerebral aneurysm: Significance of artery and aneurysm shapes (Torii et al., 2009)

Predicting the hemodynamic forces near the aneurismal site helps with understanding aneurysms better. Earlier research reports indicate that the WSS around the aneurismal site has a significant relationship with the vascular and aneurysm morphology. It was also shown statistically that the aneurysm shape (aspect ratio) is an indicator of rupture risk in cerebral aneurysm.

In this study, fluid–structure interaction (FSI) modeling of a ruptured aneurysm, two unruptured aneurysms at the middle cerebral artery (MCA) bifurcation, and a MCA bifurcation without aneurysm is carried out using vascular geometries reconstructed from CT images. We use pulsatile boundary conditions based on a physiological flow velocity waveform and investigate the relationship between the hemodynamic forces and vascular morphology for different arteries and aneurysms. The results are compared with the results obtained for the rigid arterial wall to highlight the role of FSI in the patient-specific modeling of cerebral aneurysm.

The results show that the interaction between the blood flow and arterial deformation alters the hemodynamic forces acting on the arterial wall and the interaction strongly depends on the individual aneurysm shapes. Flow impingement on the arterial wall plays a key role in determining the interaction and hemodynamic forces. When the blood flow impinges strongly on the wall, the maximum WSS tends to decrease due to the flow–wall interaction. When the blood flows straight into an aneurysm, the flow and the resulting WSS patterns are altered both qualitatively and quantitatively. When the blood in the aneurysm is nearly stagnant, a slow flow is induced by the wall motion,

which raises the minimum WSS on the aneurismal wall. The results reinforce the importance of FSI in patient specific analysis of cerebral aneurysms.

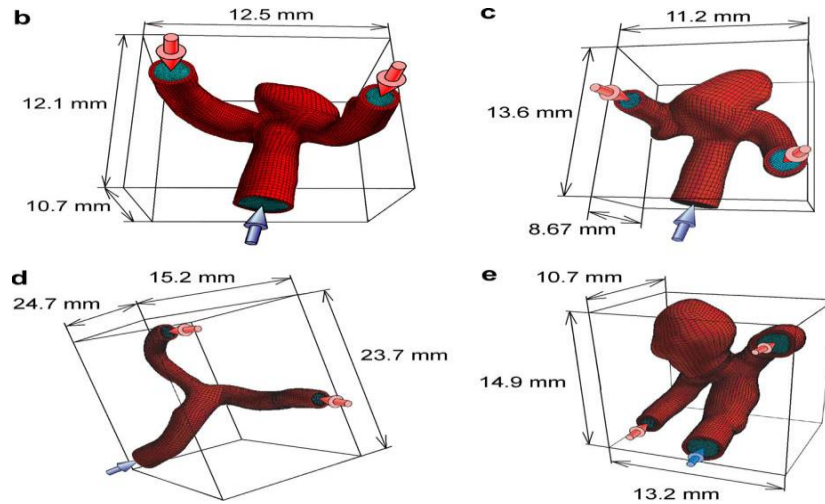


Figure 2.3: Aneurysm models based on CT images.

Source: R. Torii et al., 2009

Table 2.5: Parameters used in the simulation

Quantity	Value	Units
Diameter of the carotid artery, D_o	3.0	mm
Thickness arterial wall, t	0.3	mm
Flow rate, \dot{v}	0.1	m/s
Pressure outlet, P	10640-15960	Pa
Modulus of elasticity, E	1000000	Pa
Artery density, ρ_a	1000	kg/m ³
Blood density, ρ_b	1000	kg/m ³
Dynamic viscosity of blood, μ	0.004	kg/m. s
Poisson's ratio, ν	0.49	

Source: R. Torii et al., 2009

The inflow boundary conditions are specified as a pulsatile velocity profile prescribed by Womersley's solution of a pulsatile flow in a rigid straight pipe (Womersley, 1955). The coefficients representing physiological waveform were determined based on the waveform acquired with ultrasound Doppler at the carotid artery of a healthy volunteer in his 20's. Figure 2.5 shows the flow waveform based on the measured velocity, with the velocity profile modeled by the Womersley's formulation and the pressure waveform.

At the interface between the blood and the arterial wall, no-slip conditions are applied in the fluid mechanics part and hemodynamic forces in the structural mechanics part. Only the difference of the hemodynamic force from the level at the beginning of the cardiac cycle is applied to the arterial wall. The boundary displacements at the inlet and two outlets of the artery are set to zero. Influence of the residual stress is not taken into account.

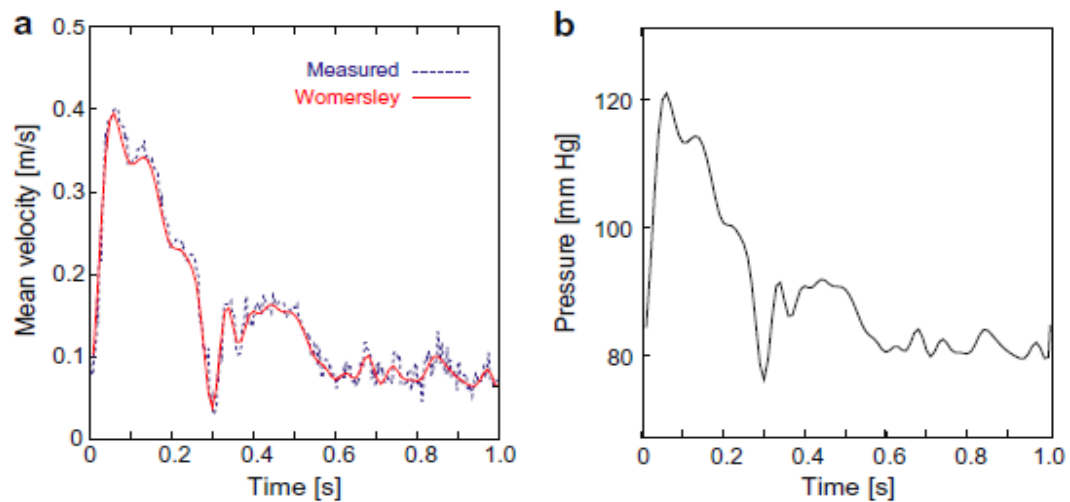


Figure 2.4: Spatial mean velocity (a) and pressure (b) waveforms.

Source: R. Torii et al., 2009

As conclusion from the data obtained, Patient-specific fluid–structure interaction (FSI) analyses were carried out for one ruptured cerebral aneurysm, two unruptured

aneurysm, and a Y-shaped bifurcation without aneurysm, all at the middle cerebral artery and reconstructed based on CT images. The results were compared with the results for the rigid arterial walls to broaden the previously acquired knowledge (Torii et al., 2007) on the importance of FSI in patient-specific simulations of cerebral aneurysms.

2.7 CONCLUSIONS

This thesis presents a review of the recent developments in the study on cerebral aneurysm. Many important, complex and interesting phenomena involving cerebral aneurysm have been reported in the literature. The use of this analysis in a wide range of applications appears promising, but the development of the field faces several challenges:

- (i) The lack of agreement between experimental results from different groups.
- (ii) The lack of theoretical understanding about the cerebral aneurysms.

Further numerical and experimental research investigations are needed to understand the initiation, growth and rupture of cerebral aneurysm and find the alternative to solve this problem for these fields.

CHAPTER 3

METHODOLOGY

3.1 INTRODUCTION

Methodology is one of the most important things to be considered in a project to ensure that the project run smoothly without any problem and to get the expected results successfully. Furthermore, the time management to finish the project can be planned more efficiency and late submission can be avoided. Besides that, if any problem occurred during the process, the time taken to solve the problem can be shortening. This is because the source of the problem can be detected easily by referring the flow of the project methodology.

In this chapter, the methodology for the project is compressed in a flow chart as shown in Figure 3.1 in order to give a clear view of the progress that need to be done to complete this final year project. For the analysis process, it is discussed in details starting from the designing of the artery, parameters set up and analysis of the model of blood flow and cerebral aneurysm. The process of Fluid-Structure Interaction is the main purpose to explain in this chapter and has been described briefly in the analysis flow chart as shown in Figure 3.2. Overall, this chapter further describes the study of Fluid-structure interaction modeling of blood flow and cerebral aneurysm.

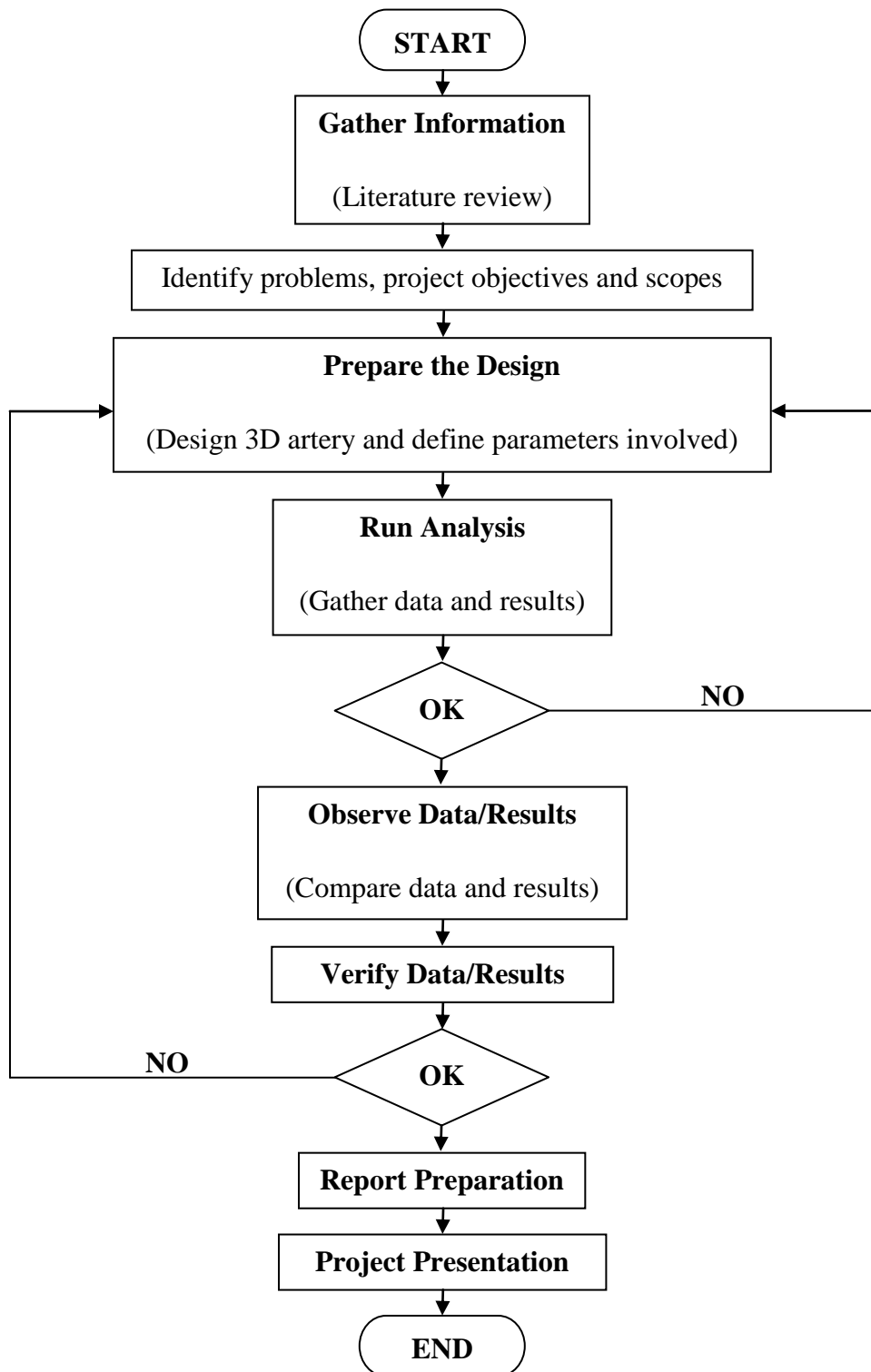


Figure 3.1: The Flow Diagram of the Project

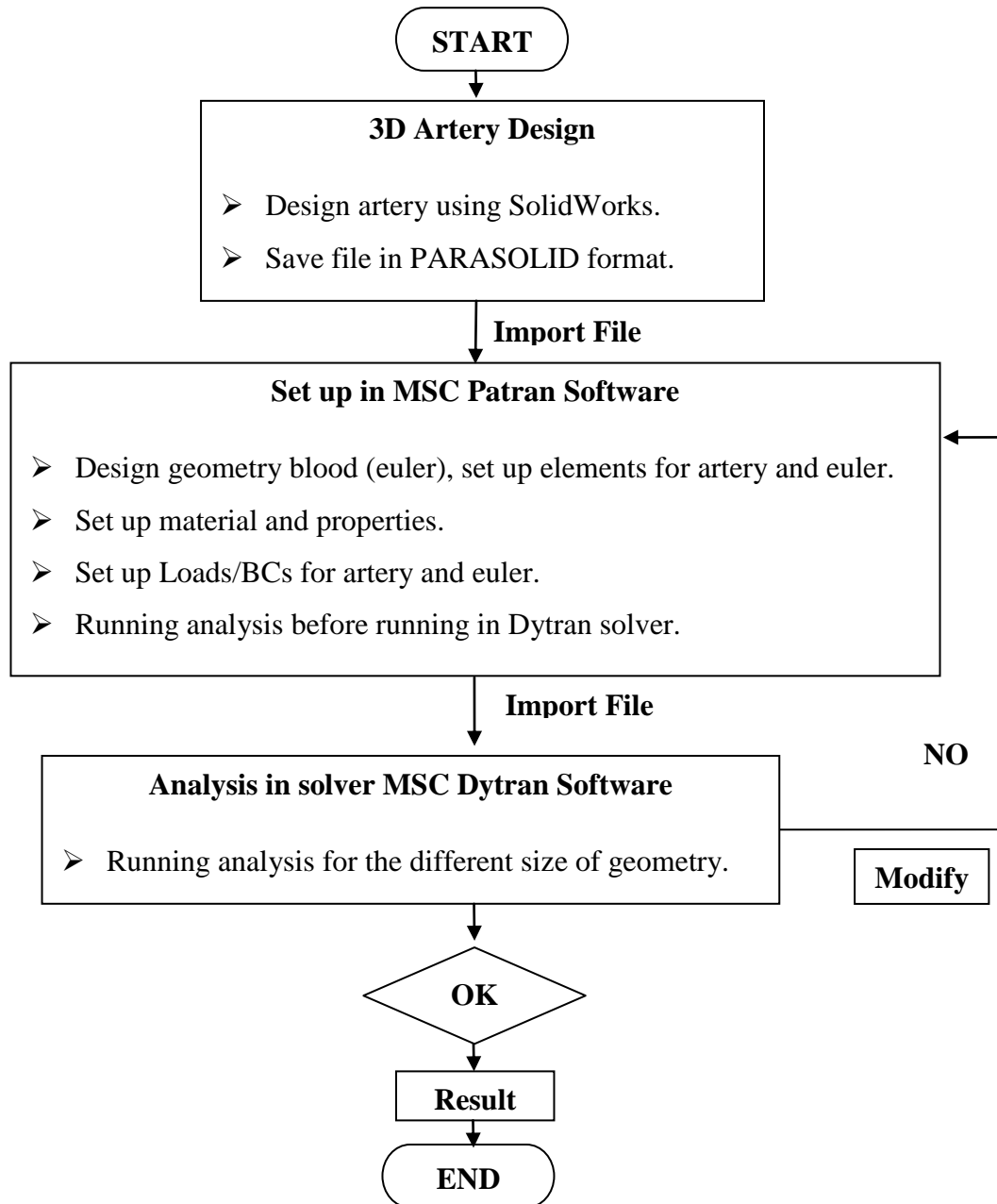


Figure 3.2: The Flow Diagram of the Analysis

3.2 SOFTWARE

In this project, three different types of engineering software are used to perform the numerical simulation of a computational model for aneurysm growth. A brief explanation of the software is discussed as below.

3.2.1 SolidWorks Software

SolidWorks is a 3D mechanical CAD (computer-aided design) program that runs on Microsoft Windows and was developed by Dassault Systèmes SolidWorks Corp., a subsidiary of Dassault Systèmes, S. A. (Vélizy, France).

SolidWorks is a parasolid-based solid modeler, and utilizes a parametric feature-based approach to create models and assemblies. Parameters refer to constraints whose values determine the shape or geometry of the model or assembly. Parameters can be either numeric parameters, such as line lengths, or geometric parameters, such as tangent. Building a model in SolidWorks usually starts with a 2D sketch (although 3D sketches are available for power users).

For this project, SolidWorks software is used to create the 3-D artery design which has the same dimension as in experimental one. This design then exported into MSC Patran software.

3.2.2 MSC Patran Software

Patran is the world's most widely used pre/post-processing software for Finite Element Analysis (FEA), providing solid modeling, meshing, and analysis setup for MSC Nastran, Marc, Abaqus, LS-DYNA, ANSYS, and Pam-Crash. Designers, engineers, and CAE analysts tasked with creating and analyzing virtual prototypes are faced with a number of tedious, time-wasting tasks. These include CAD geometry translation,

geometry cleanup, manual meshing processes, assembly connection definition, and editing of input decks to setup jobs for analysis by various solvers.

Patran provides a rich set of tools that streamline the creation of analysis ready models for linear, nonlinear, explicit dynamics, thermal, and other finite element solvers. Meshes are easily created on surfaces and solids alike using fully automated meshing routines (including hex meshing), manual methods that provide more control, or combinations of both. Finally, loads, boundary conditions, and analysis setup for most popular FE solvers is built in, minimizing the need to edit input decks.

In this project, MSC Patran software is used to create the mesh, set up material and properties, set up boundary conditions and analysis for the design.

3.2.3 MSC Dytran Software

Dytran is an explicit finite element analysis (FEA) solution for analyzing complex nonlinear behavior involving permanent deformation of structures. Dytran enables you to study the structural integrity of designs to ensure that final products stand a better chance of meeting customer safety, reliability, and regulatory requirements.

Dytran delivers a structural, material flow and coupled FSI capabilities in a single package. Dytran's explicit nonlinear solver technology is ideal for extreme, short-duration events and allows you simulate models that involve high degree of nonlinearities – material, geometric and boundary condition nonlinearities. Dytran uses a unique coupling feature that enables integrated analysis of structural components with fluids and highly deformed materials in one continuous simulation.

For this project, MSC Dytran software is used to simulate the Fluid-structure interaction modeling of cerebral aneurysm and blood flow in the artery.

3.3 STRUCTURAL ANALYSIS

The important characteristics that need to be considering in the structural analysis is geometry of cerebral aneurysm, arterial structure, finite element analysis (FEA) and material model. These characteristics can influence the result obtain in the simulation.

3.3.1 Geometry of Cerebral Aneurysm

The core of the model involves a quasi-steady approach, supported by the different scales of the local time-accurate hemodynamic, and the evolution of an aneurysm, or more. The approach entails the estimation of a prevalent hemodynamic state and subsequently the estimation of the evolution of the disease under the assumption that this state remains constant, until geometric considerations dictate a reevaluation of the hemodynamic. In this manner, we have the flexibility to account for the hemodynamic in a variety of ways. An idealized geometry of a common carotid artery was used for the application of the computational model that mimics the process described in our hypothesis.

3.3.2 Arterial Structure

Cerebral aneurysm is linked to hemodynamic in the cerebral arterial network (Steiger, 1990). In particular, the wall shear stress (WSS) plays an important role in the disease progression of aneurysm because the arterial wall remodeling is controlled by the WSS acting on the endothelium (Lehoux et al., 2002). The relationship between the blood flow, resulting WSS in the aneurismal site and vascular morphology has been investigated from various aspects.

From epidemiological point of view, aneurysm geometry characterized by the height, diameter, and neck width (or aspect ratio, $AR = \text{height}/\text{neck width}$) in Figure 2.1 is reported statistically to indicate the progression and rupture risk of aneurysms (Ujiie et

al. 1999 and Russel et al. 2003) particularly connected the aneurysm progression to blood flow stagnation owing to the aneurysm geometry.

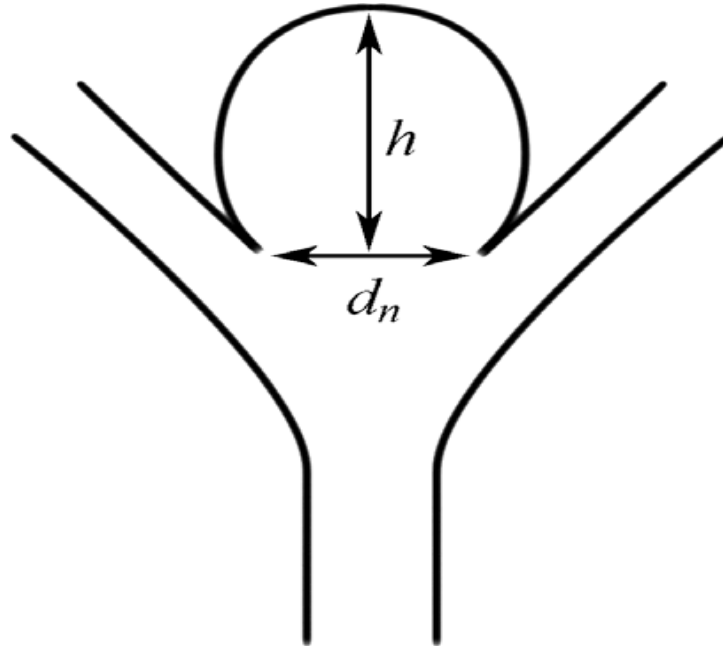


Figure 3.3: Definition of aspect ratio, $AR = h/d_n$ (h and d_n are height and neck width of the aneurysm).

Source: Ujiie et al., 1999

Detailed hemodynamic in cerebral aneurysms has been investigated experimentally (Tateshima et al., 2001) and computationally to understand better the mechanisms contributing to the aneurysm progression. However, the mechanisms causing aneurysm still remain to be unveiled. One of the main findings regarding aneurysm hemodynamic so far is the sensitivity of the blood flow to the vascular morphology. Aspect ratio of an aneurysm (Shojima et al., 2004), ratio of the aneurysm size to parent vessel diameter (Zakaria et al., 2006) and the way an aneurysm is connected to the parent vessel for examples angle, curvature and tortuosity of the parent vessel (Cebal et al., 2005) are important factors determining hemodynamic in an aneurysm.

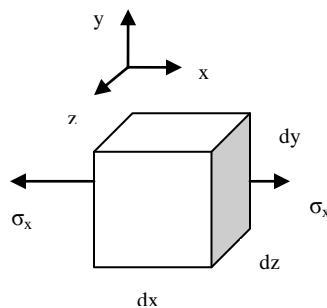
3.3.3 Finite Element Analysis (FEA)

Finite element analysis is used regularly in many engineering industries, especially the aerospace and motor industries, to accurately determine the stress distribution in complex components. Usually finite element models contain tens of thousands and possibly hundreds of thousands of elements, resulting in hundreds of thousands of (simultaneous) equations (Venkatasubramaniam et al., 2004). Certain steps in formulating a finite element analysis of a physical problem are common to all such analyses, whether structural, heat transfer, fluid flow, or some other problem. These steps are embodied in commercial finite element software packages. The steps are described as preprocessing, solution and post-processing. The preprocessing step is quite generally, described as defining the model and includes define the geometric, element types to be used, material properties, element connectivity (mesh the model), physical constraints (boundary conditions) and loadings (Hutton, 2003). During the solution phase, finite element software assembles the governing algebraic equations in matrix form and computes the unknown values of the primary field variables. Analysis and evaluation of the solution results is referred to as post-processing.

In general, the concept of normal strain is introduced and defined in the context of a uniaxial tension test. The elongated length L of a portion of the test specimen having original length L_0 (the gauge length) is measured and the corresponding normal strain defined as

$$\varepsilon = \frac{L-L_0}{L_0} = \frac{\Delta L}{L_0} \quad (3.1)$$

This is simply interpreted as ‘change in length per unit original length’ and is observed to be a dimensionless quantity.



The normal strain in the x direction at the point depicted is then

$$\varepsilon_x = \frac{dx' - dx}{dx} = \frac{\partial u}{\partial x} \quad (3.2)$$

The shear strain is

$$\gamma_{xy} = \frac{\partial u}{\partial y} + \frac{\partial v}{\partial x} \quad (3.3)$$

Where the double subscript is used to indicate the plane in which the angular change occurs. Again referring to the simple uniaxial tension test, the modulus of elasticity is defined as the slope of the stress-strain curve in the elastic region or

$$E = \frac{\sigma_x}{\varepsilon_x} \quad (3.4)$$

Poisson's ratio is defined as

$$\nu = - \frac{\text{unit lateral contraction}}{\text{unit axial elongation}} \quad (3.5)$$

Introduce the shear modulus or modulus of rigidity, defined by

$$G = \frac{E}{2(1+\nu)} \quad (3.6)$$

3.3.4 Material Model

Material model and material properties play an important role in the result of the Fluid-Structure Interaction (FSI). Choosing the right material model and material properties will improve the result. The materials parameters required depend on the types of materials being used. The parameters used in the simulation are shown in Table 3.1.

Table 3.1: Parameters used in the simulation

Quantity	Value	Units
Length of the tubular model, L	70	mm
Diameter of the artery, D_o	6.5	mm
Thickness arterial wall, t	0.35	mm
Uniform Velocity inlet, V	0.1	m/s
Uniform Pressure outlet, P	6665	Pa
Modulus of elasticity, E	120000	Pa
Blood density, ρ_b	1000	kg/m ³
Blood dynamic viscosity, μ	0.0035	kg/m. s
Poisson's ratio, ν	0.4	
Artery density, ρ_a	1000	kg/m ³

3.4 FLUID FLOW

There is a wide variety of fluid flow problems encountered in practice, and it is usually convenient to classify them on the basis of some common characteristics to make it feasible to study them in groups. There are several flow assumed to be involved in this project such as laminar and incompressible flows.

3.4.1 Flow in Artery

Flow in a tube can be laminar or turbulent, depending on the conditions of the flow. At low velocities, the flow of the fluid is laminar because it is streamlined. The flow of the fluid turns turbulent when the velocity is increased beyond a critical value. Transition from laminar to turbulent flow does not occur suddenly but it occurs over some range velocity where the flow fluctuates between laminar and turbulent flow before it becomes fully turbulent. In practice, most pipe flows occurred in turbulent while laminar flows occurs when highly viscous fluid such as blood flow and small diameter tubes.

In this project, the simulation will be assumed as laminar flow and this type of flow will be discussed in the next chapter.

3.4.2 Laminar Flow in Artery

Consider the steady laminar flow of an incompressible fluid with constant properties in the fully developed region of a straight circular tube. Obtain the momentum equation by applying a momentum balance to a differential volume element, and obtain the velocity profile by solving it. An important aspect of the analysis here is that it is one of the few available for viscous flow. The velocity profile is written as

$$u(r) = 2 V_{\text{avg}} \left(1 - \frac{r^2}{R^2}\right) \quad (3.7)$$

This is a convenient form for the velocity profile since V_{avg} can be determined easily from the flow rate information.

The maximum velocity occurs at the centerline and is determined from Eq.3.7 by substituting $r = 0$,

$$u_{\text{max}} = 2V_{\text{avg}} \quad (3.8)$$

Therefore, the average velocity in fully developed laminar tube flow is one-half of the maximum velocity.

3.4.3 Newtonian and Non-Newtonian Fluids

The study of the deformation of flowing fluids is called rheology. Newtonian fluids defined as fluids for which the shear stress is linearly proportional to the shear strain rate. Newtonian fluids are analogous to elastic solids (Hooke's Law). Many common fluids, such as air and other gases, water, kerosene, gasoline, and other oil-based liquid, are Newtonian fluids.

Fluids for which the shear stress is not linearly related to the shear strain rate are called non-Newtonian fluids. Examples include slurries and colloidal suspensions, polymer solutions, blood, paste, and cake batter. Some non-Newtonian fluids exhibit a “memory”-the shear stress depends not only on the local strain rate but also on its history. A fluid that returns (either full or partially) to its original shape after the applied stress is released is called viscoelastic.

3.4.4 Navier-Stokes Equation for Incompressible Flow

From this point on, we limit our discussion to Newtonian fluids, where by definition the stress tensor is linearly proportional to the strain rate tensor. Although the blood is known to be non-Newtonian in general, assume it to be Newtonian in this study (Womersley, 1955). Assume incompressible flow ($\rho = \text{constant}$). Assume nearly isothermal flow that local changes in temperature are small or nonexistent; this eliminates the need for a differential energy equation. A further consequence of the latter assumption is that fluid properties, such as dynamic viscosity μ and kinematic viscosity ν , are constant. With these assumptions, it can be shown that the viscous stress tensor reduces to

$$\tau_{ij} = 2\mu\varepsilon_{ij} \quad (3.9)$$

Where ε_{ij} is the strain rate tensor shows that stress is linearly proportional to strain. Navier-Stokes equation for incompressible flow with constant viscosity written as

$$\rho \frac{D\vec{V}}{Dt} = -\vec{\nabla}P + \rho\vec{g} + \mu \nabla^2 \vec{V} \quad (3.10)$$

This famous equation is named in honor of the French engineer Louis Marie Henri Navier (1785-1836) and the English mathematician Sir George Gabriel Stokes (1819-1903), who both developed the viscous terms, although independently of each

other. The Navier-Stokes equation is the cornerstone of fluid mechanics. It may look harmless enough, but it is unsteady, nonlinear, second order, partial differential equation.

3.4.5 Computational Fluid Dynamics (CFD)

Cerebral aneurysms, an abnormal outward bulging of one of the arteries in the brain, are another leading cause of death in the United State of America. Studies have attributed the origin and formation of brain aneurysms to various hemodynamic factors such as shear stress and stagnation regions. Since the formation and growth of the aneurysms is related to the hemodynamic factors, CFD studies of aneurysms can provide the required insight in formation and treatment of intracranial aneurysms. The inherent complexity of human blood flow however presents factors such as two-phase fluid dynamics (blood cells and liquids), non-Newtonian fluid dynamics, unsteadiness due to pulsed flow, and flexibility and motion of the artery walls that need approximation models to simulate using CFD.

3.5 BOUNDARY CONDITIONS

The type of flow that is modeled is determined by the imposed boundary conditions. There are several types of boundary conditions available. The most relevant ones are listed and briefly described in the following. In the description given, the words face or planes are used, implying three-dimensional flow. For a two-dimensional flow, the word edge or line should be substituted for face or plane.

3.5.1 Wall Boundary Conditions

The simplest boundary condition is that of a wall. Since fluid cannot pass through a wall, the normal component of velocity is set to zero relative to the wall along a face on which the wall boundary condition is prescribed. In addition, because of the no-slip condition, usually set the tangential component of velocity at a stationary wall to zero as well. There are situations where desire to let the fluid slip along the wall (call this an

“inviscid wall”). Note that with this simplification, the fluid is allowed to “slip” along the surface, since the viscous shear stress caused by the air above it is negligibly small. When making this approximation, surface waves and their associated pressure fluctuations cannot be taken into account.

3.5.2 Inflow/Outflow Boundary Conditions

There are several options at the boundaries through which fluid enters the computational domain (inflow) or leaves the domain (outflow). They are generally categorized as either velocity-specified condition or pressure specified condition. At a velocity inlet, specify the velocity of the incoming flow along the inlet face. At a pressure inlet, specify the total pressure along the inlet face. For example, flow coming into the computational domain from a pressurized tank of known pressure or from the far field where the ambient pressure is known.

At a pressure outlet, fluid flows out of the computational domain. Specify the static pressure along the outlet face; in many cases this is atmospheric pressure (zero gage pressure). For example, the pressure is atmospheric at the outlet of a subsonic exhaust pipe open to ambient air. Flow properties, such as temperature, and turbulence properties are also specified at pressure inlets and pressure outlets. For the latter case, however, these properties are not used unless the solution demands reverse flow across the outlet. Reverse flow at a pressure outlet is usually an indication that the computational domain is not large enough.

Pressure is not specified at a velocity inlet, as this would lead to mathematical over specification, since pressure and velocity are coupled in the equations of motion. Rather, pressure at a velocity inlet adjusts itself to match the rest of the flow field. In similar situation, velocity is not specified at a pressure inlet or outlet, as this would also lead to mathematical over specification. Rather, velocity at a pressure-specified boundary condition adjusts itself to match the rest of the flow field (Cengel and Cimbala, 2006).

3.6 FLUIDS-STRUCTURE INTERACTION

Using fluid–structure interaction (FSI) analysis, reported earlier in (Torii et al., 2006) that the dynamic change in vascular morphology and hypertensive blood pressure, which is one of the risk factors in subarachnoid hemorrhage, affects the hemodynamic. However, the importance of FSI in cerebral aneurysms is still debated because the human intracranial arteries are stiffer than the other arteries (Hayashi et al., 1980), and it was asserted in an earlier computational–angiographical study that the impact of vascular motion on the hemodynamic is not crucial (Cebal et al., 2005).

To gain a clearer view on the roles of FSI in various types of cerebral aneurysms, the results are compared to those obtained for the rigid arterial wall for the same subjects. The investigated in (Torii et al., 2007) the role of FSI in aneurysms, including two subjects with hypertensive blood pressure. This study expands the range of geometric variation to four subjects, but under normotensive blood pressure, to broaden our understandings. In particular, inclusion of a bifurcation without aneurysm would enable us to evaluate the role of FSI in aneurysms at initial stages.

The structural mechanics is governed by the force equilibrium equations and computed with the Galerkin finite element method. The arterial structure is modeled as linearly-elastic material with finite strain. Although arterial and aneurismal walls are known to be governed by complicated constitutive laws (Humphrey, 2002), it was shown in (Torii et al., 2008) by comparison between the linearly-elastic and hyper-elastic material models that the linearly-elastic material model would be able to present the trends in displacement patterns. The fluid and structural mechanics systems are coupled at the interface by kinematic and dynamic conditions. The two systems are solved with a block-iterative coupling approach (Tezduyar et al. 2006 and Tezduyar, 2004). The fluid mesh is updated by using an automatic mesh moving method (Tezduyar et al., 1993), where the motion of the nodal points is governed by the equations of elasticity.

3.7 MODELING OF THE ARTERY

The different size of geometry carried out the different result of wall deformation. Therefore, the initial geometry is compared to the other geometry with the different thicknesses. The SolidWorks software is used to design a 3D cylinder with a dimension of 0.55 mm in thickness, 6.5 mm in diameter and 70 mm in length as shown in Figure 3.4. This cylinder represents the artery that is used in the analysis. The designs of the artery geometry are repeated with the 0.45 mm and 0.35 mm in thickness as shown in Figure 3.5 and Figure 3.6.

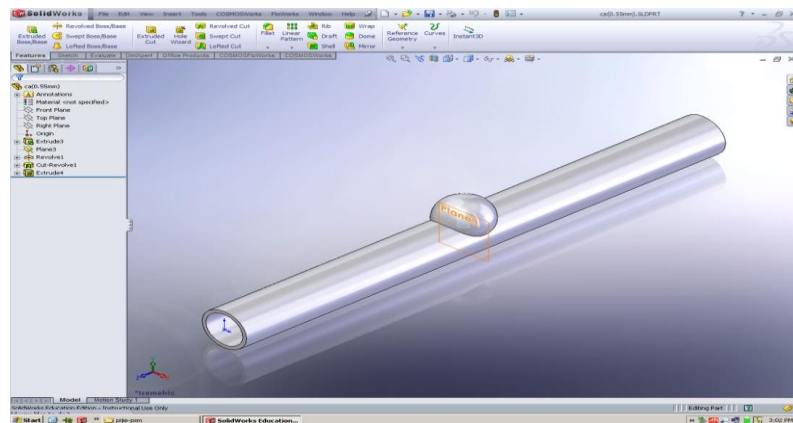


Figure 3.4: 3D artery for 0.55 mm thickness

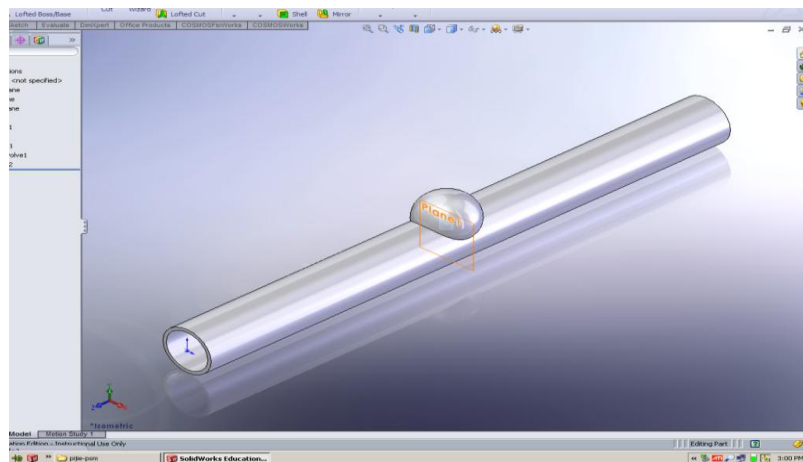


Figure 3.5: 3D artery for 0.45 mm thickness

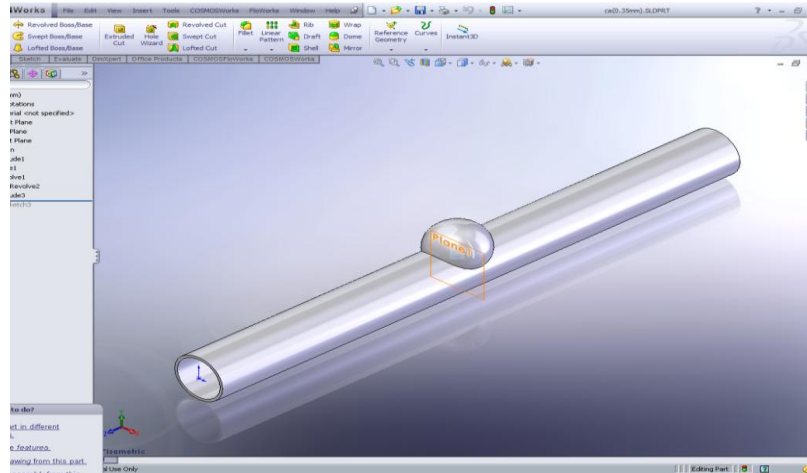


Figure 3.6: 3D artery for 0.35 mm thickness

3.8 CONCLUSIONS

This chapter discussed about the structure of cerebral aneurysm and the implementation of boundary condition. The information of loading and material of cerebral aneurysm is needed to develop the model and to analyze into the MSC Dytran software. This software is combination of FEA, CFD and FSI analysis. Research is needed to given much attention on FSI analysis of cerebral aneurysms.

CHAPTER 4

RESULTS AND DISCUSSIONS

4.1 INTRODUCTION

This chapter discuss about the result obtained from the numerical simulation of computational model for aneurysm growth using MSC Dytran software. The objective of this chapter is to determine the relationship of the wall deformation and the different thickness of geometry were used. In this analysis, the selection of the mesh type, the selection of material, properties and loading or boundary condition are very important.

Firstly, the simulations were carried out on to check the reliability and accuracy of the numerical methods and parameter setting in the MSC Patran software. After that, the simulations are carried out using MSC Dytran software and the data obtained from both simulations are used to make proper comparison between aneurysm and blood flow.

All the evaluated data from the simulations are then calculated and present as non-dimensionless result and graph. The results from these simulations are also compared with the results from the experiment along with the discussion.

4.2 NUMERICAL SIMULATION MODELING

In this study, the model for cerebral aneurysm growth is generated using three software which are SolidWorks, MSC Patran and MSC Dytran. SolidWorks software is used to design the artery for the fluid flows through it. The dimension for this artery

condition is 0.35 mm in thickness, 6.5 mm in diameter and 70 mm in length. The result from SolidWorks is shown in Figure 4.1 below.

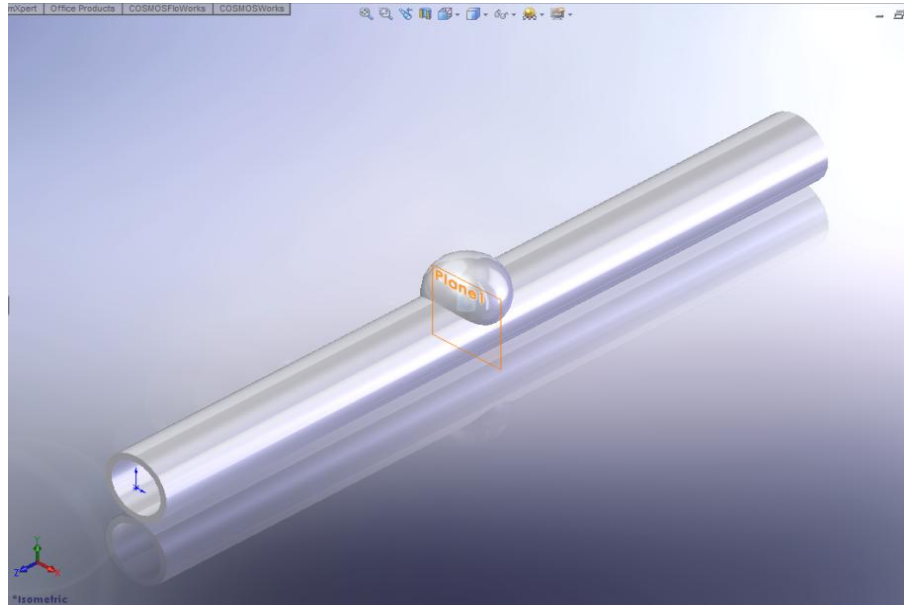


Figure 4.1: The design of 3D artery in SolidWorks

Figure 4.1 above shows the design of the artery used in the simulation. The steps for design the artery is repeated with the different size of geometry which is 0.45 mm and 0.55 mm in thickness.

The second software used in this simulation is MSC Patran. MSC Patran is used to build the mesh and to set up the boundary condition, material and properties for the artery and blood (euler) and described as pre-processing stage. This software also used to draw the blood (eulerian solid). The artery and the euler after the meshing process in MSC Patran is shown in Figure 4.2 and Figure 4.3.



Figure 4.2: The aneurysm design after the meshing process

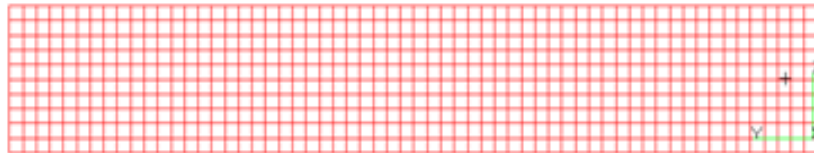


Figure 4.3: The euler design after the meshing process

The mesh for artery design contains 953 nodes and 2856 elements. The type of mesh used is Tet 4 with automatic global edge lengths. The mesh for euler design contains 7381 nodes and 6000 elements. The type of mesh used is Hex 8 with 0.05 global edge lengths. This type of mesh gave accurate result and does not encounter any error during the analysis process.

The third software used to simulate the cerebral aneurysm growth is MSC Dytran. MSC dytran uses a unique coupling feature that enables integrated analysis of structural components with fluids and highly deformed material in one continuous simulation and described as post-processing stage. For this project, MSC Dytran software is used to simulate the Fluid Structure Interaction (FSI) modeling of cerebral aneurysm and blood flow.

4.3 MATERIAL PROPERTIES

The material properties for artery and blood used in the simulation are calculated from the experimental result. Table 4.1 below shows the material properties used in the simulation.

Table 4.1: Material properties used in the simulation

Quantity	Value	Units
Length of the tubular model, L	70	mm
Diameter of the artery, D_o	6.5	mm
Thickness arterial wall, t	0.35	mm
Velocity inlet, V	0.1	m/s
Pressure outlet, P	6665	Pa
Modulus of elasticity, E	120000	Pa
Blood density, ρ_b	1000	kg/m ³
Poisson's ratio, ν	0.4	
Artery density, ρ_a	1000	kg/m ³

4.4 ARTERIAL AND ANEURYSM WALL DEFORMATION

From the simulation process, the result can be obtained and shows in visualization of the flow as shown in Figure 4.4. The figure shows result of the flow in the cerebral aneurysm for the thickness is 0.35 mm and the inner diameter is 6.15 mm. The results of this research which is the maximum displacement of the aneurysm wall, the wall shear stress (WSS), the maximum velocity change in aneurysm and the maximum pressure distribution were obtained as the main result of simulation. In aneurysm region, all phenomena were not constant due to the diameter and thickness changes in aneurysm. The local wall displacement is the relevant variable to access the local aneurysm growth. The wall shear stress (WSS) was considered as stress measured to resume the effect on the wall under multi axial loading condition. The result obtained from the simulation is record as shown in the Table 4.2 with the different in thickness and inner diameter.

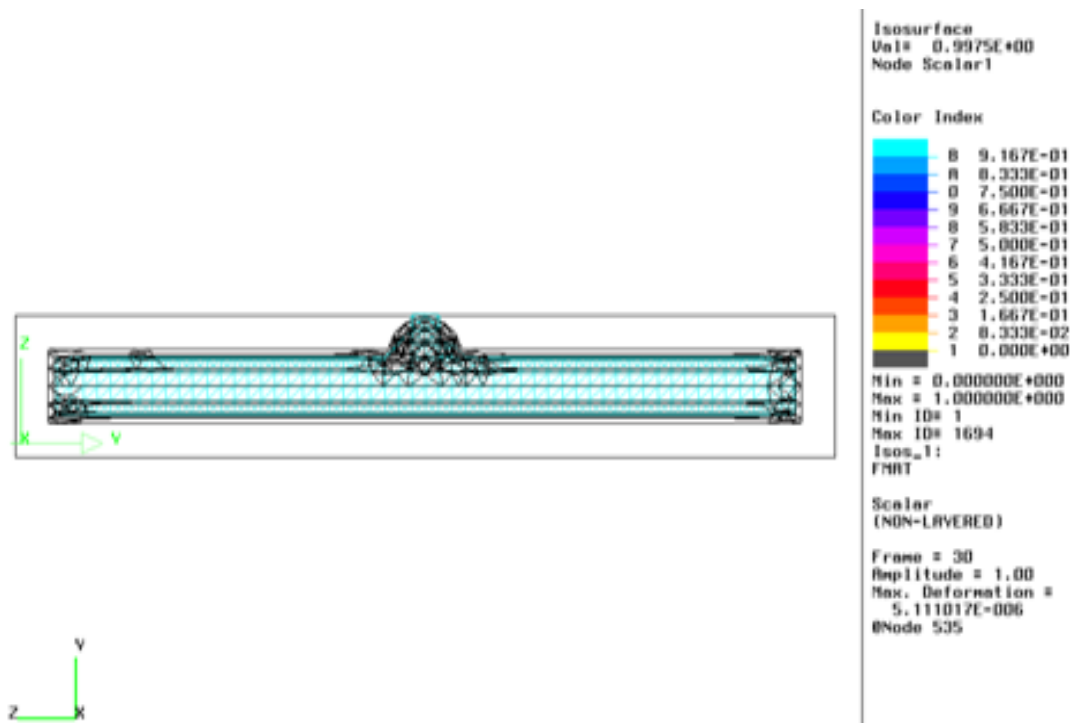


Figure 4.4: The flow in the cerebral aneurysm for thickness 0.35 mm and inner diameter 6.15 mm

Table 4.2: Result of the simulation

Inner Diameter of cerebral aneurysm (mm)	Thickness of cerebral aneurysm (mm)	Max Velocity (m/s)	Max Pressure (Pa)	Max Displacement (mm)
5.95	0.55	0.04114	15572	0.005078
6.05	0.45	0.14977	13696	0.005094
6.15	0.35	0.28584	11264	0.005111

The displacement is evident near the bifurcation for all cases. The aneurysm wall contributes an important role in the progression of aneurysm (Torii et al., 2008). The maximum displacement is 0.005111 mm for the thickness 0.35 mm and the inner diameter 6.15 mm as shown in Figure 4.5. They occur at the peak systole in all cases (Torii et al., 2009). The maximum displacement is indicated with a circle in the figure. The simulation was repeated with the different value of thickness and inner diameter. The value which is 0.45 mm in thickness and 6.05 mm in inner diameter and 0.55 mm in thickness and 5.95

mm in inner diameter respectively. The maximum displacement value for both cerebral aneurysms wall is 0.005094 mm and 0.005078 mm respectively as shown in Table 4.2. The pattern indicates elongation where the displacement is the maximum at the peak and gradually decreases toward the neck. From the result shown the maximum displacement of wall increase when the diameter of cerebral increase. This is because the diameters of cerebral influence the blood flow in cerebral. Thus, the displacement at the neck aneurysm decreases due to the slower blood flow. The result shows that the displacement of wall depends on the wall thickness and the diameter of cerebral aneurysm. The artery and aneurysm wall expand because of the blood pressure. In generally, the distribution of displacement location is depending on the aneurysm shape and volume. The blood pressure forces the wall of aneurysm until it cannot withstand any more pressure. The walls become weak and injured, and then it ruptures. The graph of the maximum displacement and maximum velocity against the thickness of the cerebral aneurysm is plotted in the Figure 4.6 and the graph of the maximum displacement and maximum velocity against the inner diameter of the cerebral aneurysm is plotted in the Figure 4.7.

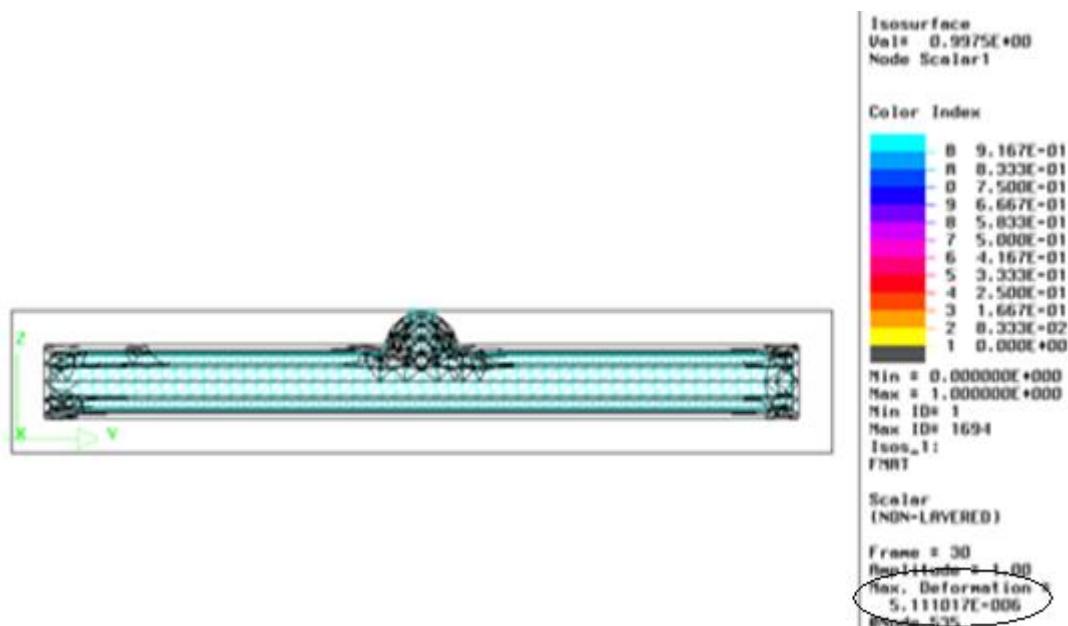


Figure 4.5: Maximum displacement of cerebral aneurysm for thickness 0.35 mm and inner diameter 6.15 mm

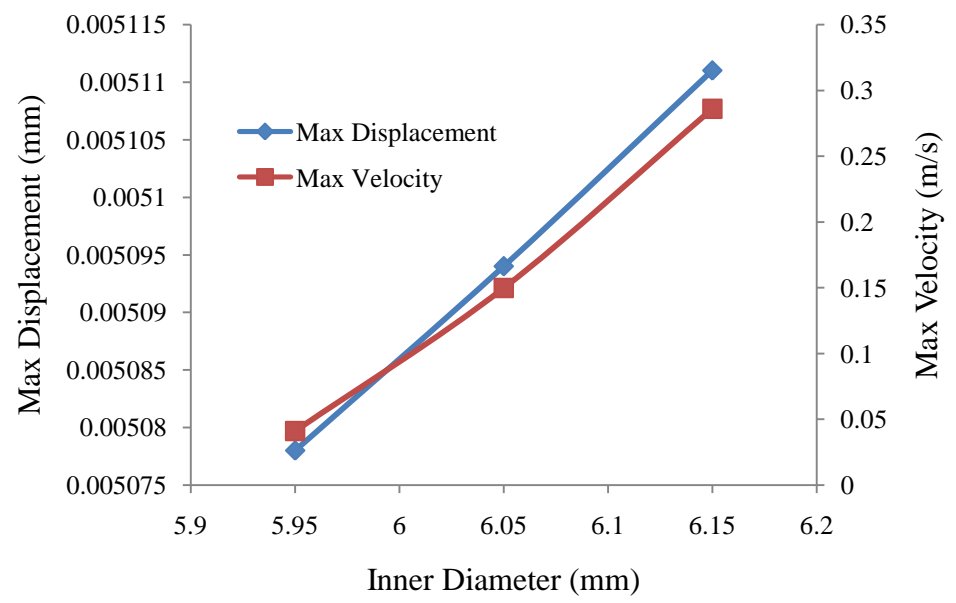


Figure 4.6: Graph of the maximum displacement and maximum velocity against inner diameter

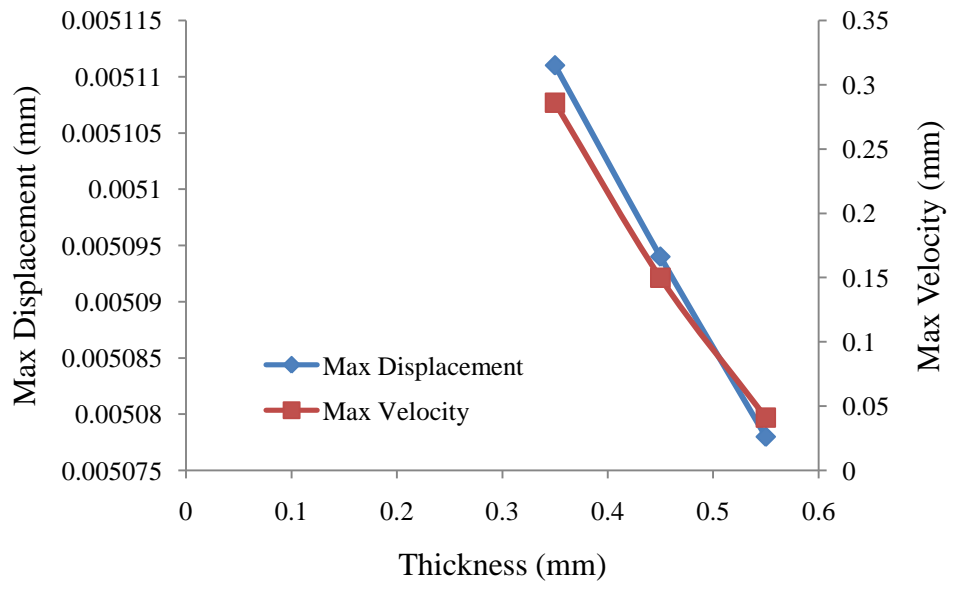


Figure 4.7: Graph of the maximum displacement and maximum velocity against thickness

4.5 WALL SHEAR STRESS

The most interesting hemodynamic parameter in relation to the aneurysm progression is the wall shear stress (WSS). It varies in time due to the pulsation of the flow waveform as shown in Figure 4.8 and Figure 4.9. The maximum value generally occurs at the peak systole when the inflow becomes the maximum. The wall shear stress patterns at the various stages during the aneurismal growth are shown in visualization in Figure 4.10. The results show that the maximum wall shear stress at the peak systole which is indicated with a circle in the figure is 0.9167 Pa for the thickness 0.35 mm and the inner diameter 6.15 mm. These results coincide and justify the observation that the shear stress presents with higher values at the neck neighborhood (Banerjee et al., 1996). The wall shear stress profile for the different diameters is varying by the interaction between the blood flow and arterial wall deformation. The wall shear stress on the aneurismal wall playing an important role in the progression of aneurysm follows the same trend as the above-mentioned maximum wall shear stress.

The flow-wall interaction also varies quantitatively the wall shear stress profile on the aneurysm. The wall shear stress after the peak systole shows focal high value on the wall and the wall shear stress is very low near the apex. Low wall shear stress occurring near the apex is known to play a role in rupture of aneurysm through degradation of the aneurismal wall (Ujiie et al., 1999) because very low wall shear stress results in abnormal metabolic activity in arterial wall (Steiger, 1990). The maximum wall shear stress for the thickness 0.45 mm and inner diameter 6.05 mm is 1.1078 Pa and the maximum wall shear stress for thickness 0.55 mm and inner diameter 5.95 mm is 1.1683 Pa were recorded in Table 4.3. The result shows that the maximum wall shear stress is decreased when the diameter of cerebral aneurysm is increased and the location is not constant and varies with pulse cycle. The maximum wall shear stress is observed towards the neck during peak systole and it decreases with declaration of pulse. The nature of variation of wall shear stress shows the pulsatile behavior (Abdul Khader et al., 2009). The graph of maximum wall shear stress against inner diameter of cerebral aneurysm and the graph of maximum wall shear stress against thickness are plotted as shown in Figure 4.11 and Figure 4.12.

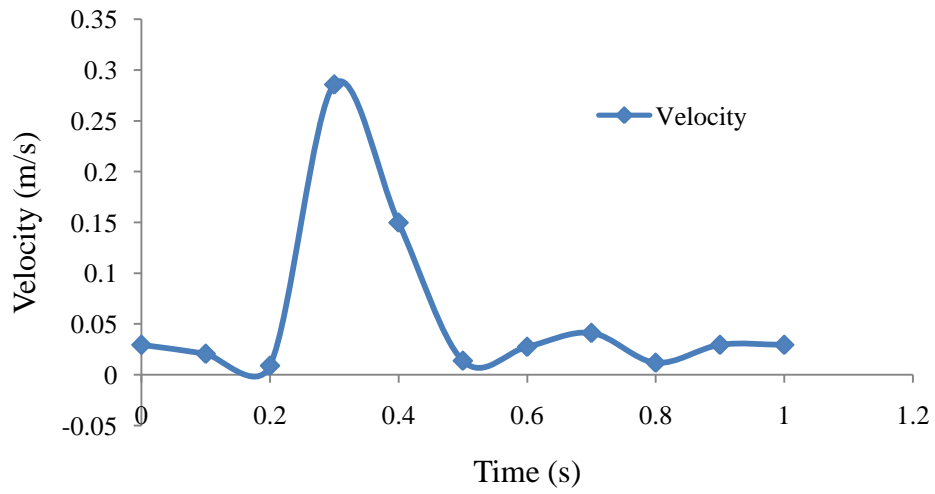


Figure 4.8: The inlet velocity waveforms

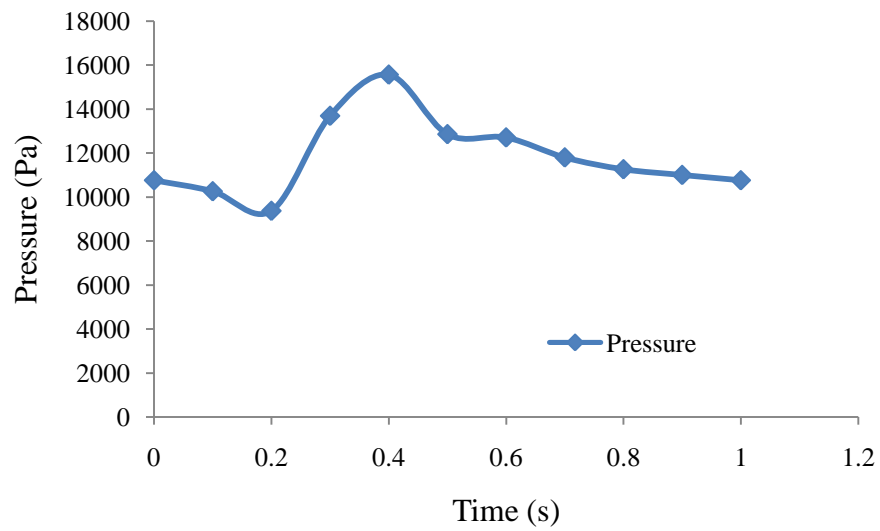


Figure 4.9: The outlet pressure waveforms

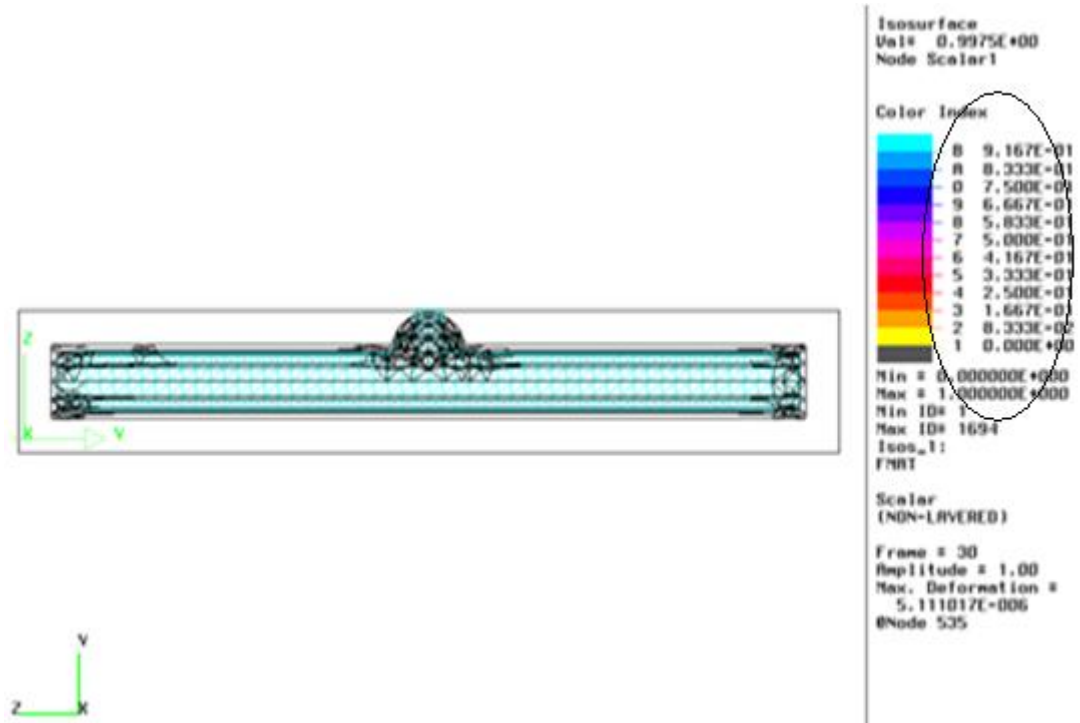


Figure 4.10: Wall shear stress of cerebral aneurysm thickness 0.35 mm and inner diameter 6.15 mm

Table 4.3: Maximum wall shear stress for cerebral aneurysm

Inner Diameter of Cerebral aneurysm (mm)	Thickness of Cerebral aneurysm (mm)	Max Wall Shear Stress (Pa)
6.15	0.35	0.9167
6.05	0.45	1.1078
5.95	0.55	1.1683

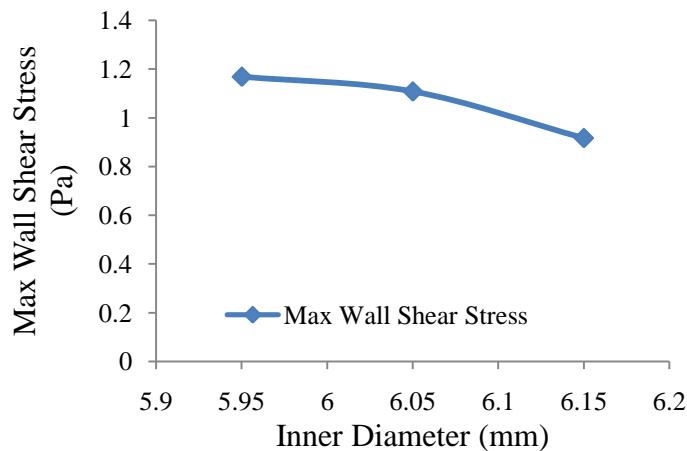


Figure 4.11: The graph of maximum wall shear stress against inner diameter

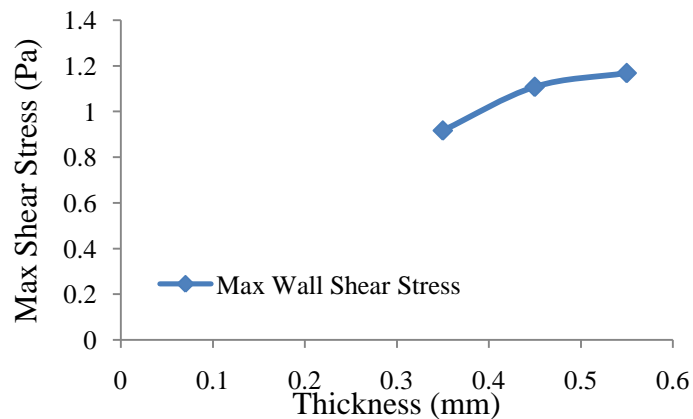


Figure 4.12: The graph of maximum wall shear stress against thickness

4.6 INTERACTION BETWEEN THE BLOOD FLOW AND WALL DEFORMATION

The velocity of the flow gives effect to the wall displacement in cerebral aneurysm. The velocity profile shown are the effect of the wall deformation on the wall shear stress profile since the interaction between the blood flow and arterial wall dynamics is reflected to the wall shear stress through the velocity profile. The flow from the inlet proceeds in the parent artery and extend on the wall at the neck of the aneurysm. The graph maximum displacement against the velocity changes and the pressure distribution

were plotted to show the interaction between the blood flow and wall deformation as shown in Figure 4.13. Besides that, the dynamic interaction between flow and wall may influence the predicted pressure distribution value of this study. The wall shear stress in the extend region is only slightly higher than the other part. Hence the wall shear stress on the aneurysm is very low independent of the flow-wall interaction. This indicates that in terms of high wall shear stress, the FSI is insignificant. The impingement flow velocity near the neck of the aneurysm is smaller for compliant case because of the different structure of cerebral and axial direction.

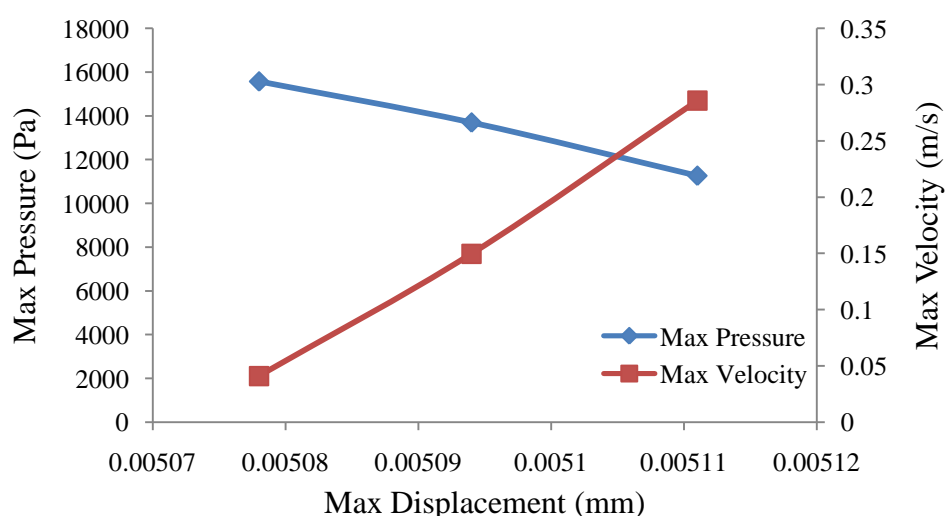


Figure 4.13: Graph of the maximum pressure and maximum velocity against maximum displacement

All the peak pressure is occurred at the neck wall while minimum pressure is outside the cerebral wall. At systolic peak, fluid pressure was found to be higher at the distal neck, demonstrating the effect of a compliant wall in combination with the characteristics of the pressure and velocity waveforms. It has shown that pressures and stresses present in an aneurysm are highly dependent not only on the size, but also the shape and symmetry of the aneurysm.

4.7 CONCLUSIONS

The Fluid Structure Interaction between the artery and the blood flow had been presented. The mesh convergence, materials and properties was set up using FEA to determine the best parameters to be used in FSI. Results obtained in this study are compared with the previous experimental and found in close agreement between them. From the results, the displacement of the wall increased when the diameter of the cerebral increased. The wall shear stress on the aneurismal is playing an important role in the progression of aneurysm. The velocity and pressure of the flow also gives effect to the wall displacement in cerebral aneurysm.

CHAPTER 5

CONCLUSIONS AND RECOMMENDATIONS

5.1 INTRODUCTION

This chapter concludes the development of the project. The outcome of the project is related to the scope and objective of the project. From that, the project is determined whether its objective was achieved or not. The future development were also stated and described. Whereas the practical refinement is explain in further detail as it vital to be carried in next project. Apart from that, the finding also include for reviews. This chapter was outline to begin with conclusion and recommendations.

5.2 CONCLUSIONS

A computational model for the growth of cerebral aneurysm had been developed. The study on FSI are involved the displacement of the aneurysm wall, wall shear stress, pressure and velocity of flow in the cerebral aneurysm. The results show that the role of FSI depends on the shape of the aneurysm, particularly on the region of flow extended and the displacement pattern in individual arterial geometry. The wall shear stress on the aneurismal is playing an important role in the progression of aneurysm. The maximum wall shear stress is 0.9167 Pa for the inner diameter 6.15 mm, 1.1078 Pa for the inner diameter 6.05 mm and 1.1683 Pa for the inner diameter 5.95 mm. The maximum wall shear stress is decreased when the diameter of cerebral aneurysm is increased. Due to overall complexity, specific choices in term of dimension and constitutive behavior are required. Thus, the aneurysm diameter is the important criteria to investigate. The maximum displacement is 0.005111 mm for the inner

diameter 6.15 mm, 0.005094 mm for the inner diameter 6.05 mm, 0.005078 mm for the inner diameter 5.95 mm. The wall displacement increased when the diameter of cerebral is increased. The aneurysm have tendency for rupture if the velocity of flow is increased. This is because the factor should be considerable is the diameter of cerebral and the thickness of wall cerebral. Studying the mechanical properties in real cerebral aneurysm would be done to get better result from the simulation. Also the good software simulation should be the good simulation to analyze the behavior of this mechanical study about the cerebral aneurysm.

5.3 LIMITATION

The real shapes of cerebral are quite different and more complicated one. Actual cerebral aneurysm's generally has even more complex shapes and has no planes of symmetry. This is different with in this study that has a symmetric axis and smooth surface contact. Besides that, the assumptions that mechanical properties like the thickness are uniform along the surface had been made. This is not realistic and influences the result of this study. The software application is the important thing to simulate the model. MSC Dytran software is having limitation to investigate the behavior of cerebral aneurysm but this software still can investigate the phenomena in cerebral aneurysm.

5.3 RECOMMENDATIONS

In order to improve this study for a computational model of cerebral aneurysm growth some recommendation is produce as below;

- a) Suitable geometry needed for the software to run smoothly without error.
- b) Set up the meshing, loading and material properties appropriately.
- c) Use actual modeling of cerebral aneurysm.
- d) Consider the flow of velocity of cerebral aneurysm.
- e) Study and learn more about the function of MSC Patran software and MSC Dytran software.

REFERENCES

- Amstrong, L. (undated). Side effects of aneurysm (online). <http://www.livestrong.com/article/> (22 Jan 2010).
- Burleson, A.C., Strother, C.M. and Turitto, V.T. 1995. *Computer modeling of intracranial saccular and lateral aneurysms for the study of their hemodynamics*, *Neurosurgery* **37**: 774–783.
- Caro, C.G., Fitzgera, J.M. and Schroter, R.C. 1969. Arterial wall shear and distribution of early atheroma in man. *Nature* **223** (5211), 1159.
- Cebral, J.R., Castro, M.A., Burgess, J.E., Pergolizzi, R.S., Sheridan, M.J. and Putman, C.M. 2005. *Characterization of cerebral aneurysms for assessing risk of rupture by using patient-specific computational hemodynamics models*, *Am. J. Neuroradiol.* **26**: 2550–2559.
- Cengel, Y.A. and Cimbala, J.M. 2006. *Fluid Mechanics: Fundamentals and applications*. New York: McGraw-Hill Companies, Inc.
- Chatziprodou, I., Tricoli, A., Poulidakos, D. and Ventikos, Y. 2007. Haemodynamics and wall remodeling of a growing cerebral aneurysm: A computational model. *Journal of Biomechanics* **40**: 412-426.
- Foutrakis, G.N., Yonas, H. and Scwabasi, R.J. 1999. *Saccular aneurysm formation in curved and bifurcating arteries*, *Am. J. Neuroradiol.* **20**: 1309–1317.
- Hayashi, K., Handa, H., Nagasawa, S., Okumura, A. and Moritake, K. 1980. *Stiffness and elastic behavior of human intracranial and extracranial arteries*, *J. Biomech.* **13**: 175–184.
- Humphrey, J.D. 2002. *Cardiovascular solid mechanics, Cells, Tissues, and Organs*. New York: Springer Verlag.
- Hutton, D.V. 2003. *Fundamentals of Finite Element Analysis*. Pullman, WA: International Edition.
- Lehoux, S., Tronc, F. and Tedgui, A. 2002. *Mechanisms of blood flow-induced vascular enlargement*, *Biorheology* **39**: 319–324.
- Lindsay, K. 2007. 3.3 Vascular Diseases (*Aneurysm*).
- Resnick, N., Yahav, H., Shay-Salit, A., Shushy, M., Schubert, S., Zilberman, L.C.M. and Wofovitz, E. 2003. Fluid shear stress and the vascular endothelium: *for better and for worse*. *Progress in Biophysics and Molecular Biology* **81** (3), 177–199.
- Russel, S.M., Lin, K., Hahn, S.A. and Jafar, J.J. 2003. Smaller cerebral aneurysms producing more extensive subarachnoid hemorrhage following rupture: *a*

radiological investigation and discussion of theoretical determinants, J. Neurosurg. **99**: 248–253.

Schievink, W.I. *Intracranial aneurysms.* N Engl J Med 1997. **336** :28–40.

Shojima, M., Oshima, M., Takagi, K., Torii, R., Hayakawa, M., Katada, K., Morita, M. and Kirino, T. 2004. Magnitude and role of wall shear stress on cerebral aneurysm: *Computational fluid dynamic study of 20 middle cerebral artery aneurysms, Stroke.* **35**: 2500–2505.

Steiger, H.J. 1990. Pathophysiology of development and rupture of cerebral aneurysms, *Acta Neurochir. Suppl.* **48**: 1–57.

Tateshima, S., Murayama, Y., Villablanca, J.P., Morino, T., Takahashi, H., Yamauchi, T., Tanishita, K. and Vinuela, F. 2001. *Intraaneurysmal flow dynamics study featuring an acrylic aneurysm model manufactured using a computerized tomography angiogram as a mold, J. Neurosurg.* **95**:1020–1027.

Texon, M., 1990. The hemodynamic basis of atherosclerosis. *Texas Heart Institute Journal* **17** (4), 355.

Tezduyar, T.E. 2004. Finite element methods for fluid dynamics with moving boundaries and interfaces, in: E. Stein, R. De Borst, T.J.R. Hughes (Eds.), *Encyclopedia of Computational Mechanics*, vol. 3: Fluids, Chapter 17, John Wiley & Sons.

Tezduyar, T., Aliabadi, S., Behr, M., Johnson, A. and Mittal, S. 1993. *Parallel finite-element computation of 3D flows, Computer* **26**: 27–36.

Tezduyar, T.E., Behr, M., Mittal, S. and Johnson, A.A. Computation of unsteady incompressible flows with the finite element methods – space–time formulations, iterative strategies and massively parallel implementations, in: *New Methods in Transient Analysis*, PVP-vol. 246/AMD-vol. **143**, ASME.

Tezduyar, T.E., Sathe, S., Keedy, R. and Stein, K. 2006. Space–time finite element techniques for computation of fluid–structure interactions, *Comput. Methods Appl. Mech. Engrg.* **195**: 2002–2027.

Torii, R., Oshima, M., Kobayashi, T., Takagi, K. and Tezduyar, T.E. 2006. Fluid structure interaction modeling of aneurysmal conditions with high and normal blood pressures, *Comput. Mech.* **38**: 482–490.

Torii, R., Oshima, M., Kobayashi, T., Takagi, K. and Tezduyar, T.E. 2007. Numerical investigation of the effect of hypertensive blood pressure on cerebral aneurysm - *dependence of the effect on the aneurysm shape, Int. J. Numer. Methods Fluid* **54**: 995–1009.

- Torii, R., Oshima, M., Kobayashi, T., Takagi, K. and Tezduyar, T.E. 2008. Fluid–structure interaction modeling of a patient-specific cerebral aneurysm: *influence of structural modeling*, *Comput. Mech.* **43**: 151–159.
- Torii, R., Oshima, M., Kobayashi, T., Takagi, K. and Tezduyar, T.E. 2009. Fluid–structure interaction modeling of blood flow and cerebral aneurysm: *Significance of artery and aneurysm shapes*. *Comput. Methods Appl. Mech. Engrg.* **198**: 3613–3621.
- Ujiie, H., Tachibana, H., Hiramatsu, O., Hazel, A., Matsumoto, T., Ogasawara, Y., Nakajima, H., Hori, T., Takakura, K. and Kajiya, F. 1999. Effects of size and shape (aspect ratio) on the hemodynamics of saccular aneurysms: *a possible index for surgical treatment of intracranial aneurysms*, *Neurosurgery* **45**: 119–130.
- Van Gijn, J. and Rinkel, G.J.E. 2001. Subarachnoid heamorrhage: *Diagnosis, cause and management*, *Brain* **124**: 249–278.
- Venkatasubramaniam, A. K., Fagan, M. J., Mehta, T., Mylankal, K. J., Ray, B., Kuhan, G., Chetter I. C. and McCollum, P. T. 2004. A Comparative Study of Aortic Wall Stress Using Finite Element Analysis for Ruptured and Non-ruptured Abdominal Aortic Aneurysms. *Eur J Vasc Endovasc Surg* **28**, 168–176.
- Womersley, J.R. 1955. *Method for the calculation of velocity, rate of flow and viscous drag in arteries when the pressure gradient is known*, *J. Physiol.* **127**: 553–563.
- Zakaria, H., Yonas, H. and Robertson, A.M. 2006. *Analysis of the importance of the ratio of aneurysm size to parent artery diameter on hemodynamic condition*, *J. Biomech.* **39**: S272.
- Ziegler, T., Bouzourene, K., Harrison, V.J., Brunner, H.R. and Hayoz, D. 1998. Influence of oscillatory and unidirectional flow environments on the expression of endothelin and nitric oxide synthase in cultured endothelial cells. *Arteriosclerosis Thrombosis and Vascular Biology* **18** (5), 686–692.
- Ziegler, T., Harrison, V.J., Brunner, H.R. and Hayoz, D. 1997. Influence of oscillatory and unidirectional flow on nitric oxide synthase in cultured endothelial cells. *Hypertension* **30** (4), 46.

APPENDIX A

MANUAL USER FOR MSC PATRAN AND MSC DYTRAN SOFTWARE APPLICATION

1. Simulation for Structure and Fluid

Open File Menu and click New. Type aneurysm under file name and click OK. Select MSC.Dytran for Analysis Code and click OK as shown in Figure 6.1.

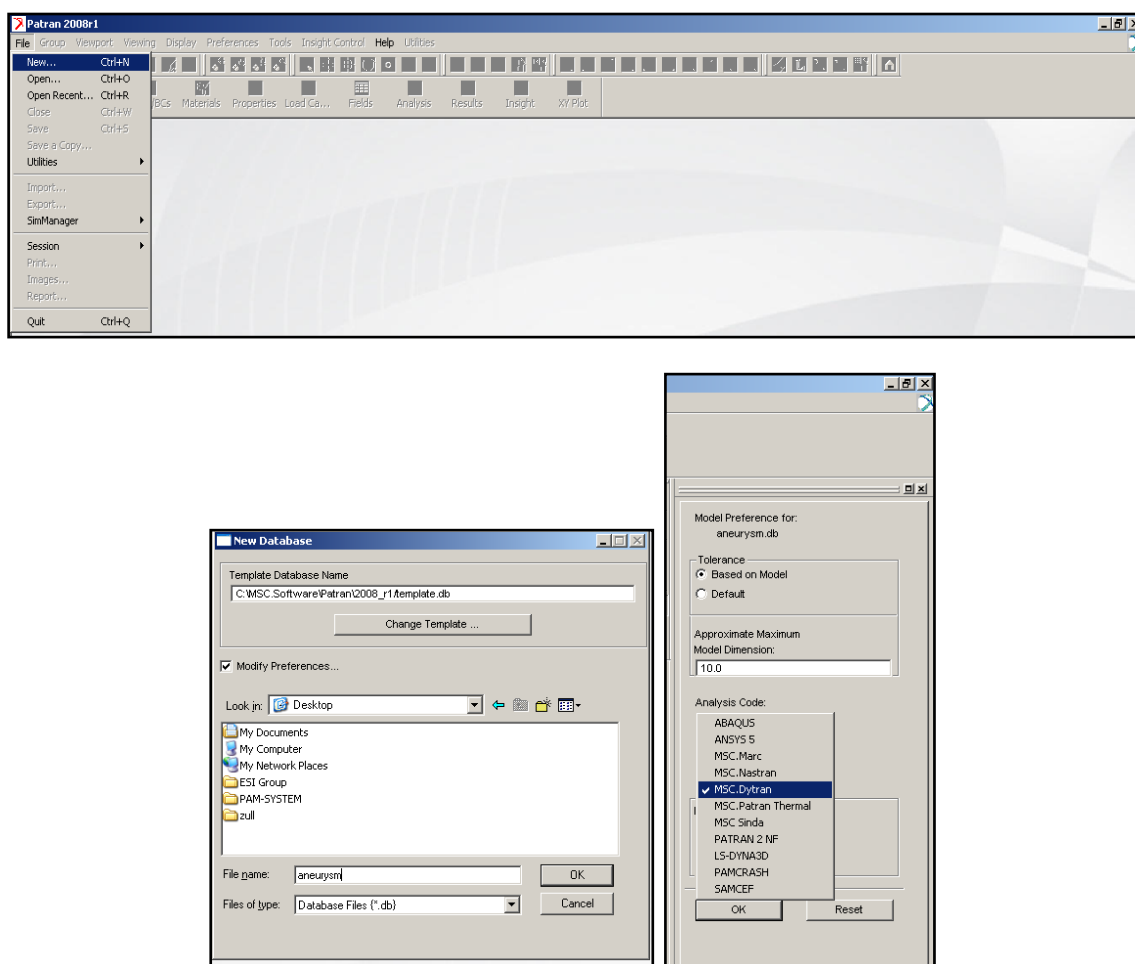


Figure 6.1: Open new database

Select Group / Create / Select Entity. Enter artery for New Group Name. Click Apply and then Cancel as shown in Figure 6.2. Click the File menu, select Import, select Parasolid xmt for Source, select artery.x.t and click Apply as shown in Figure 6.3.

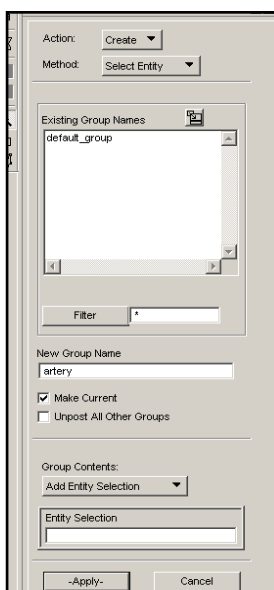
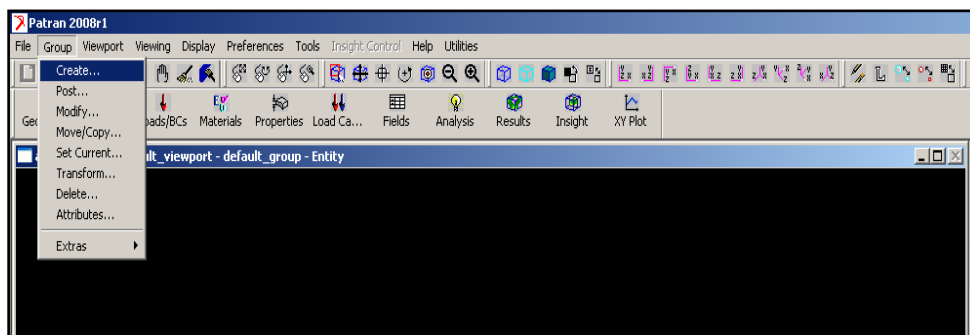


Figure 6.2: Create group for artery

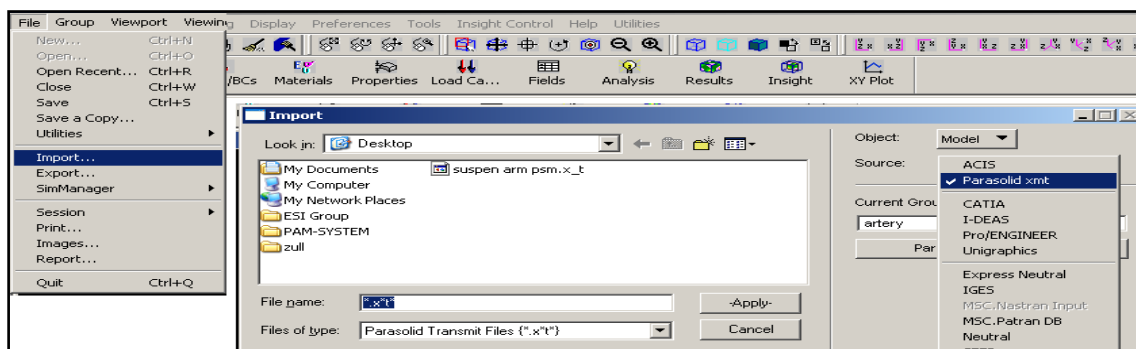


Figure 6.3: Import Parasolid xmt file

Select Group / Create / Select Entity. Enter euler for new Group name, click apply and then cancel. Select Geometry / create / solid / XYZ. Enter <0.5 0.5 -3> for vector coordinate list. Enter [-0.25 -0.25 0.12] for origin coordinates list and click apply as shown in Figure 6.4. Select Geometry / create / coord / 3 point. Enter coord 0 for refer coordinate frame, enter [-0.2 -0.2 0.1] for origin, enter [-0.2 1 0.1] for point on axis 3 and enter [1 -0.2 0.1] for point on plane 1-3 and then click apply as shown in Figure 6.5.

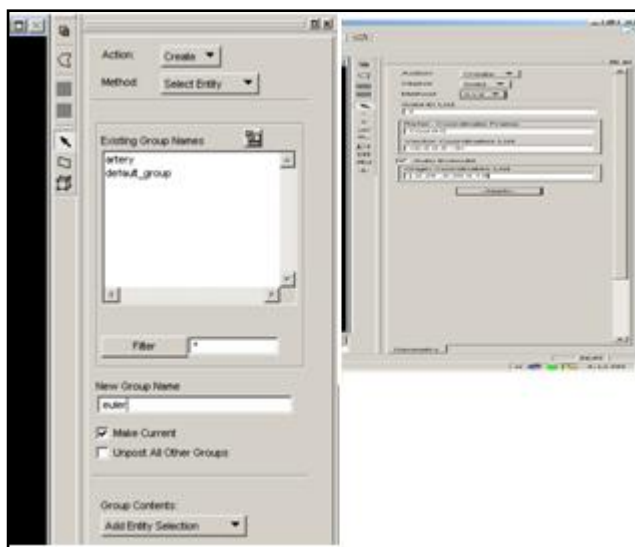


Figure 6.4: Create the eulerian region

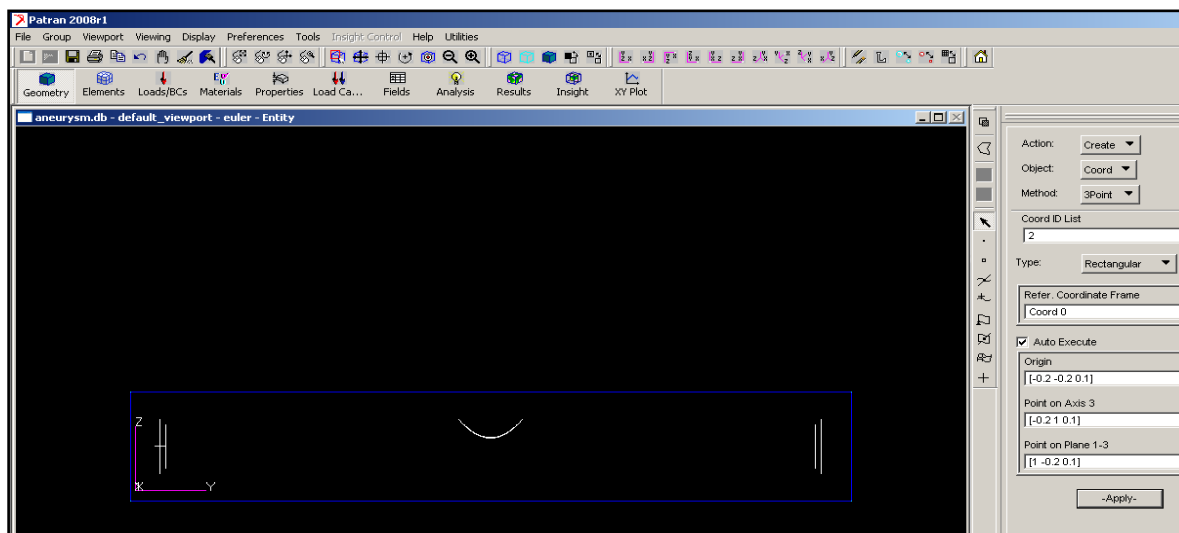


Figure 6.5: Create local coordinate system

Select Group / artery. Select artery, clicks apply and then cancel as shown in Figure 6.6. Select Elements / create / mesh / solid. Select Tet / Tetmesh / Tet 4, select solid 1 and then click apply as shown in Figure 6.7.

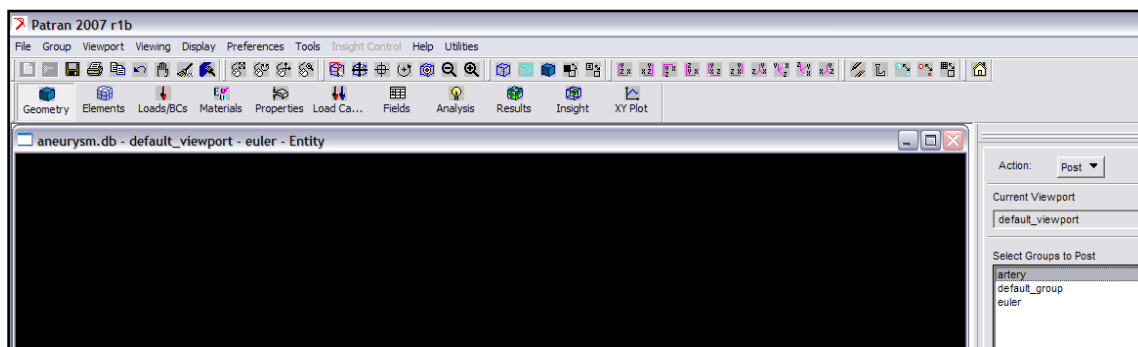


Figure 6.6: Post artery

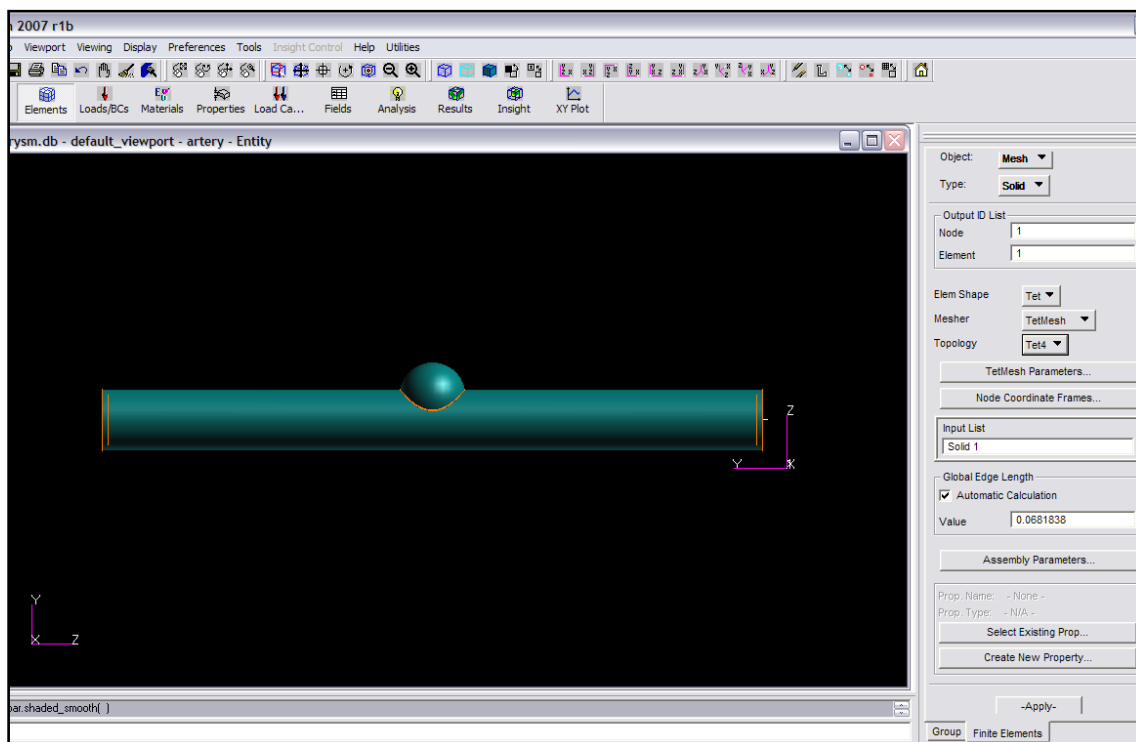


Figure 6.7: Create finite element mesh for artery

Select elements / equivalence / all / tolerance cube. Enter 0.005 for equivalencing tolerance and click apply as shown in Figure 6.8. Select Group / post, select euler and click apply and then cancel. Select Elements / create / mesh / solid as shown in Figure 6.9. Select Hex / Isomesh / Hex8, select solid 2 for solid list. Enter 0.05 for global edge length value and click apply.

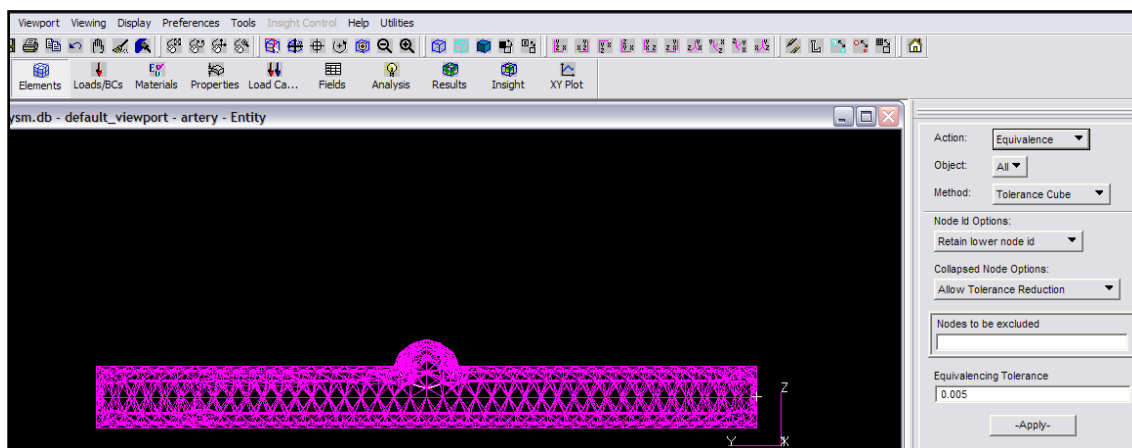


Figure 6.8: Elements equivalence

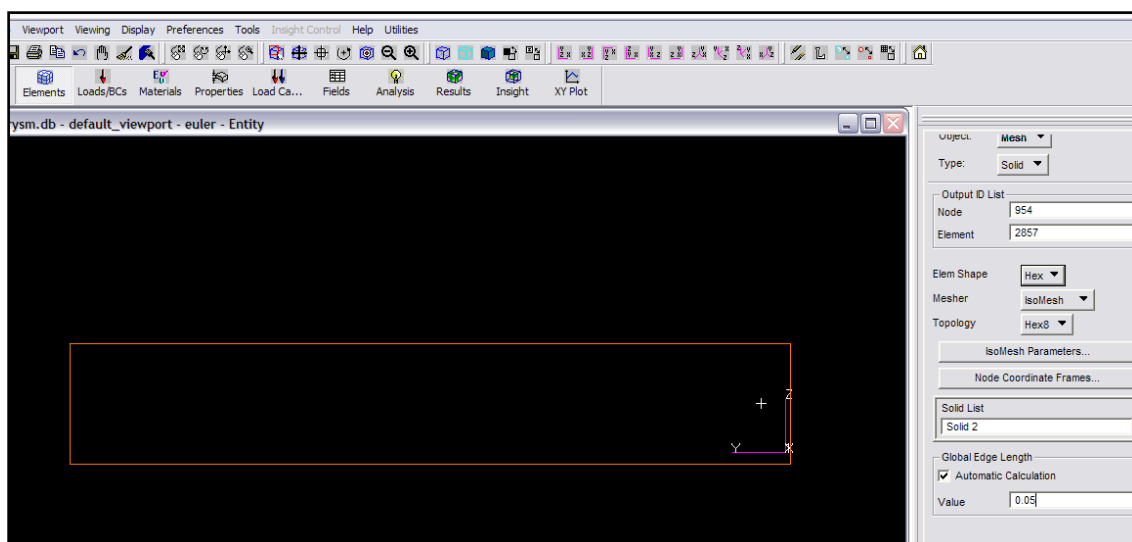


Figure 6.9: Create finite element for eulerian solid

Select Materials / create / isotropic / manual input as shown in Figure 6.10. Enter aneurysm for material name. Click input properties and select linear elastic. Enter 120000 for elastic modulus, 0.4 for Poisson Ratio, and 1000 for density click OK and click apply. Select Material / create / isotropic / manual input as shown in Figure 6.11. Enter blood for material name. Select Linfluid(DMAT) / eulerian solid (hydro). Enter 1000 for density and 2.2e9 for bulk modulus. Click OK and then click apply.

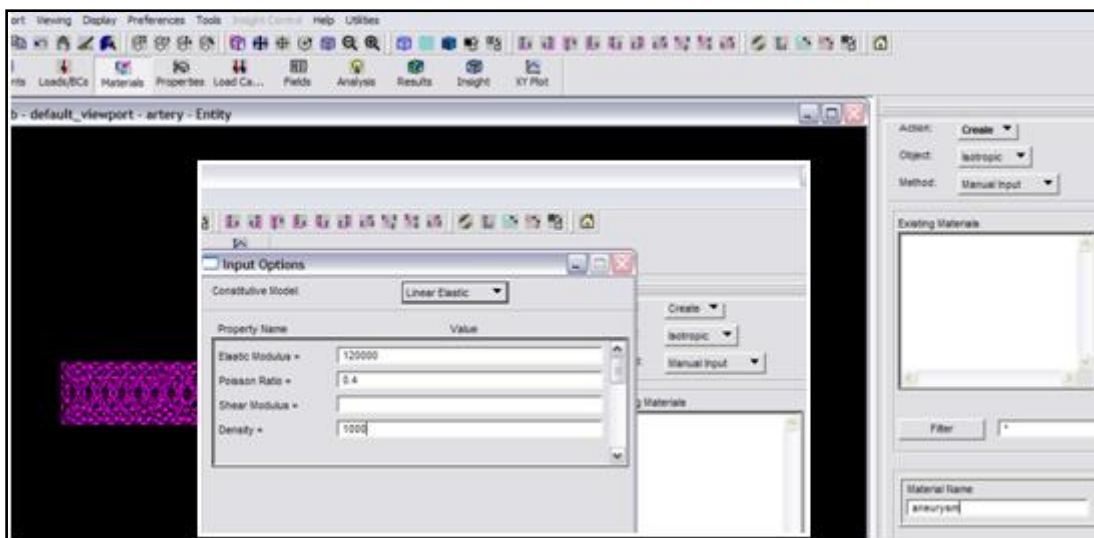


Figure 6.10: Create material for artery

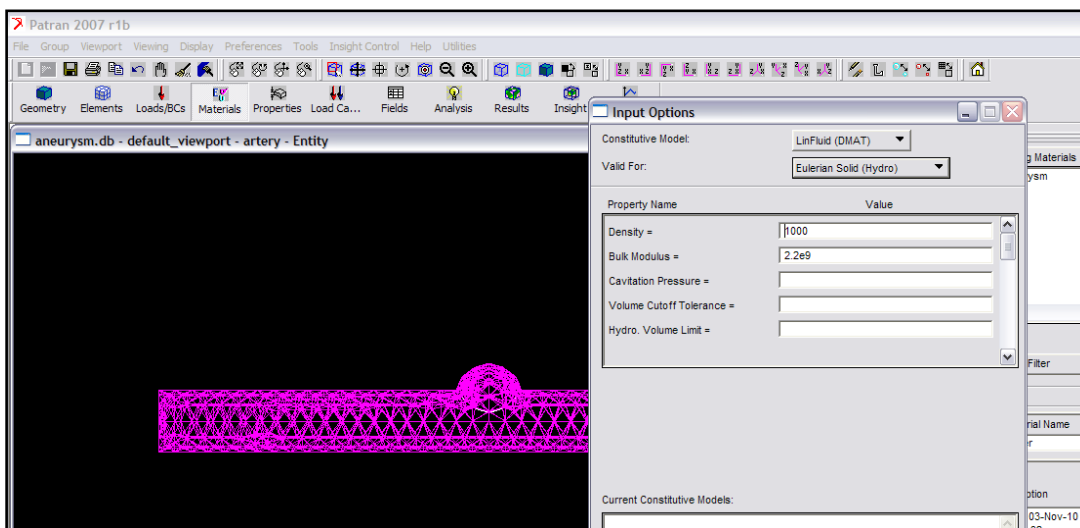


Figure 6.11: Create material for eulerian solid

Select Group / post as shown in Figure 6.12. Select artery, clicks apply and then cancel. Select Properties / create / 3D / lagrangian solid. Click input properties, select aneurysm for material name, select application region and select solid 1. Clicks add and clicks apply. Select Properties / create / 3D / eulerian solid as shown in Figure 6.13. Select hydro (peuler1), click input properties and click OK. Select application region, select solid 2 and click add and then click apply.

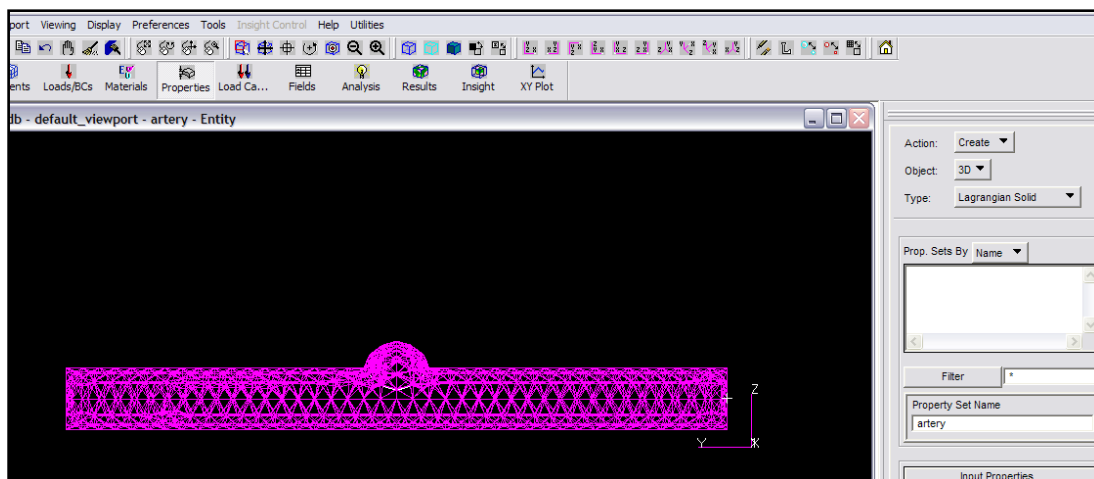


Figure 6.12: Create properties for artery

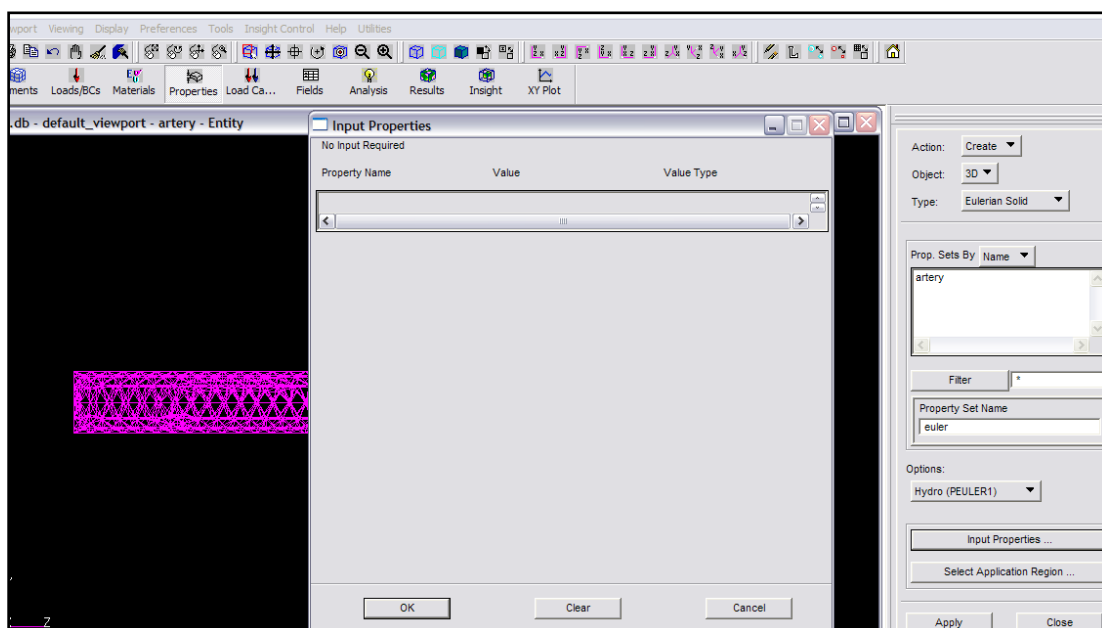


Figure 6.13: Create properties for eulerian solid

Select Loads/BCs / create / displacement / nodal as shown in Figure 6.14. Enter aneurysm_boundary for new set name. Click input data, enter $\langle 0 \ 0 \ 0 \rangle$ for both translations and rotations and click OK. Click select application region, select FEM. Pick the nodes at the edge of the artery, click add, click OK and then click apply. Select Loads/BCs / create / planar rigid wall / nodal as shown in Figure 6.15. Enter contact for new set name. Click input data and enter coord 1 for centroid orientation, clicks OK. Click select application region, select FEM for geometry filter, select all nodes for select nodes, click add and then OK and click apply.

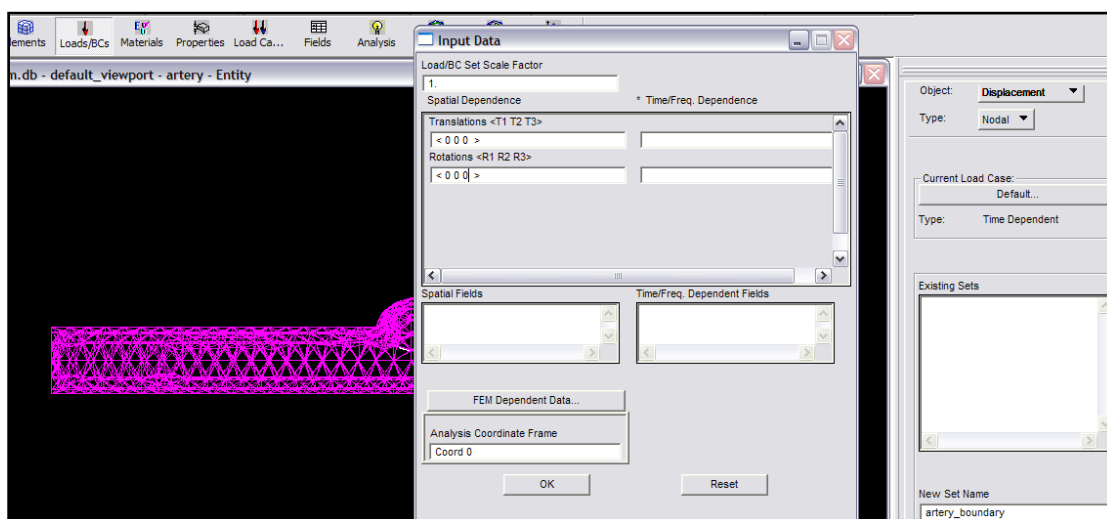


Figure 6.14: Create displacement nodal

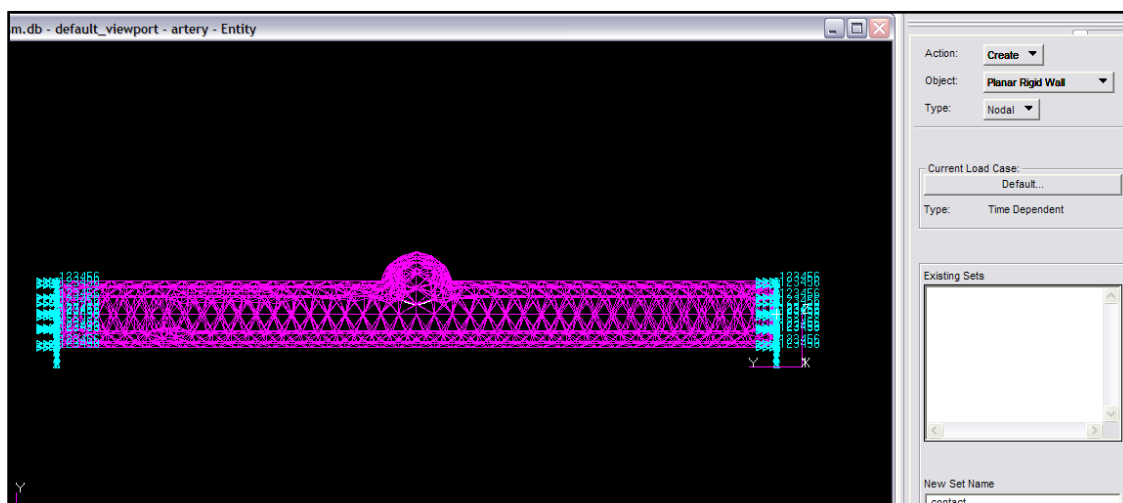


Figure 6.15: Create planar rigid wall

Select Group / post as shown in Figure 6.16. Post euler, click apply and then cancel. Select Loads/BCs / create / in. cond. Euler / element uniform / shape. Enter blood_shape, click input data, select element for shape and click OK. Click select app region, select FEM for geometry filter, select the top 8 rows, click add and OK and click apply. Repeat the same step for void_shape and select the 2 rows at the below. Select Group / post as shown in Figure 6.17. Select artery, click apply and then cancel. Select Loads/BCs / create/in. cond. Euler / element uniform / initial values. Enter blood_initial for new set name. Click input data, select blood for select euler material, enter <0 0 0.1> for initial material velocity, 1000 for density, click OK and click apply.

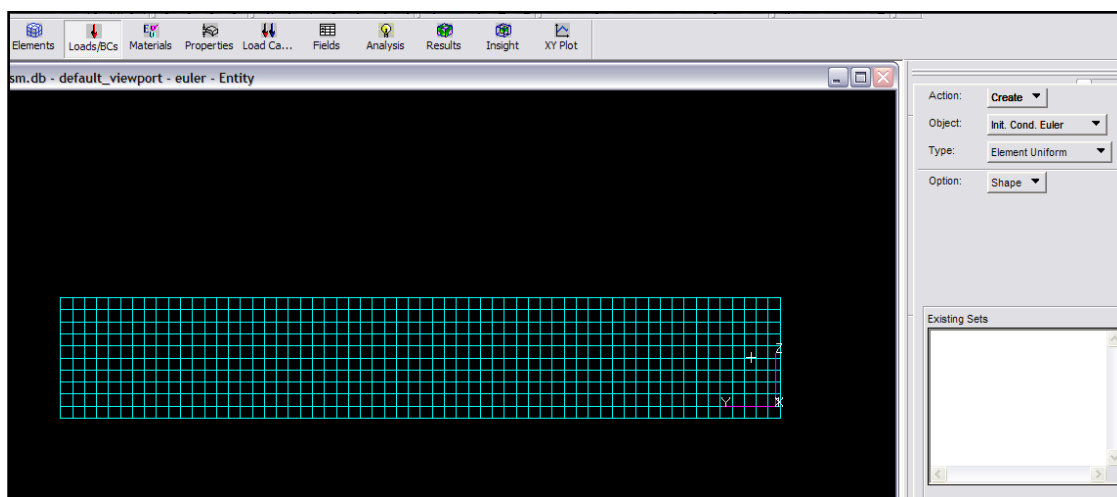


Figure 6.16: Initial condition euler for shape

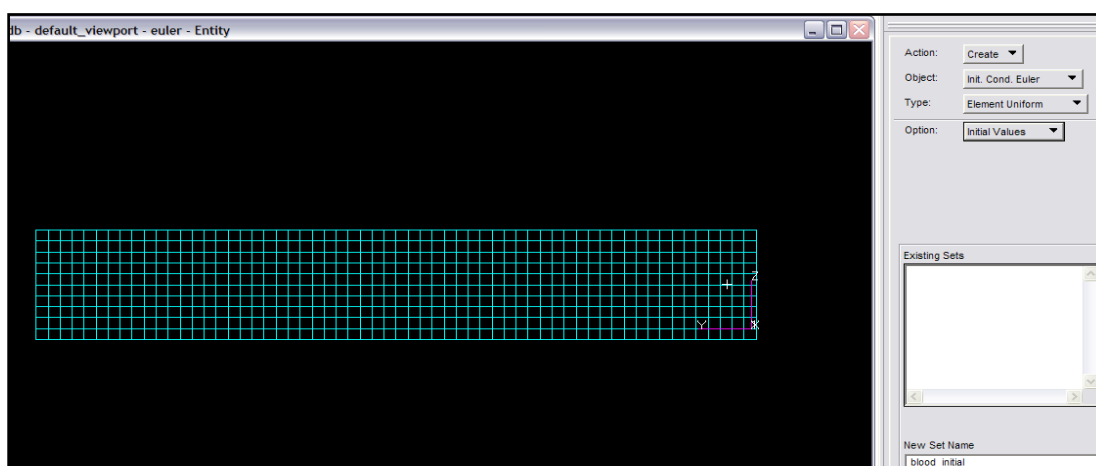


Figure 6.17: Initial condition euler for initial value

Select Loads/BCs / create / in. cond. Euler / element uniform / region definition as shown in Figure 6.18. Enter euler_region for new set name. Click input data, select euler for existing peuler1, select void_shape for existing shape sets. Enter 1 for level indicator, click add row, select euler for existing peuler1, select blood_shape for existing shape sets and select blood_initial for existing initial values set. Enter 2 for level indicator, click add row, click OK and click apply. Select Loads/BCs / create / flow / element uniform as shown in Figure 6.19. Enter flow for new set name, click input data and select both for flow type. Select blood for select material and enter <0 0 0.1> for veloc at boundary, 6665 for press at the boundary, 1000 for the density. Select app region, select FEM for geometry filter, select solid 2.6 for select 3D element faces. Clicks add and click OK and then click apply.

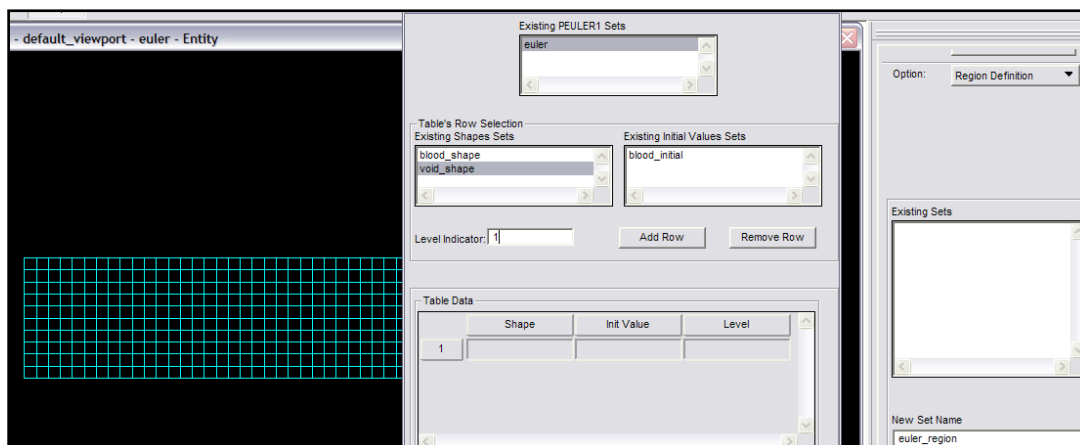


Figure 6.18: Create region definition

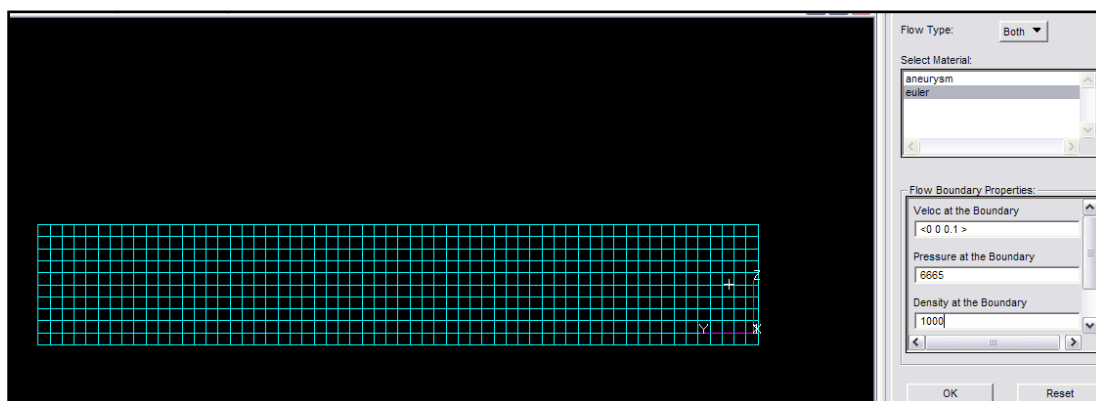


Figure 6.19: Create flow

Select Loads/BCs / create / coupling / element uniform / general as shown in Figure 6.20. Enter couple for new set name. Click input data and select outside for cover. Click OK, click select app region, select 3D for element type, select FEM for geometry filters, selects all elements. Clicks add and OK and click apply. Select Analysis / analyze / input deck / translate as shown in Figure 6.21. Click execution controls, click execution control parameters. Enter data as above and click OK. Click coupling parameters, select active for fast coupling and click ok.

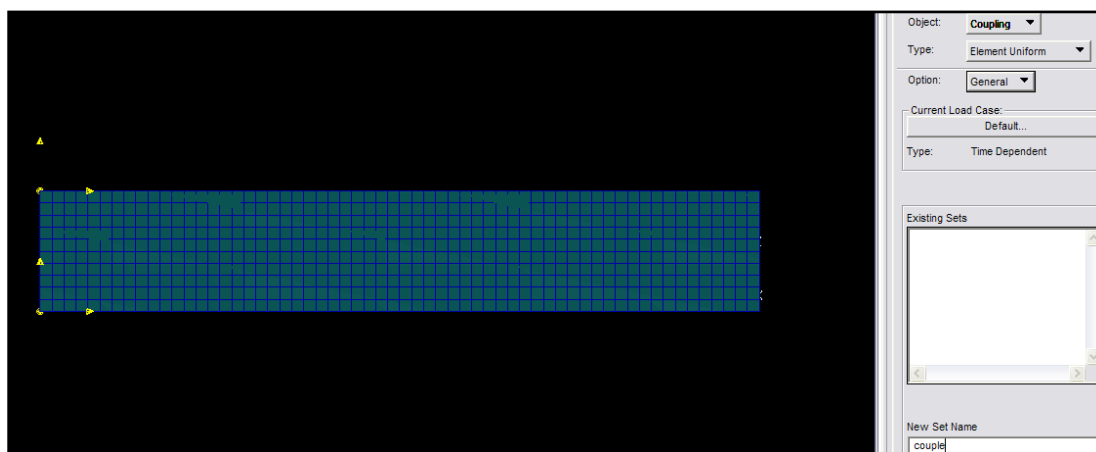


Figure 6.20: Create general coupling

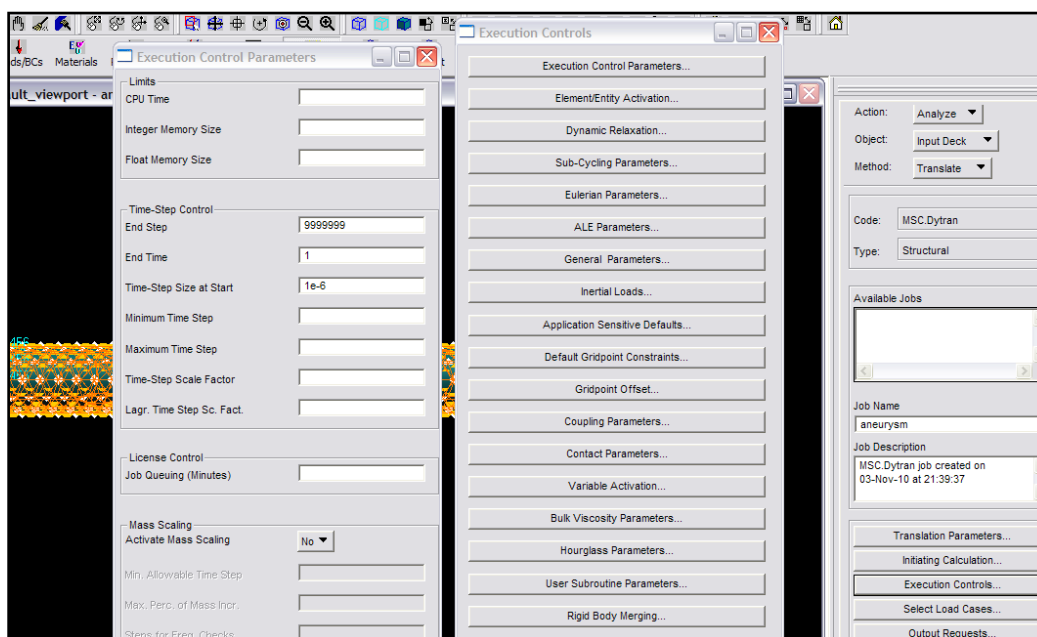


Figure 6.21: Analysis in patran

Click output request as shown in Figure 6.22. Enter data as below for the artery. Repeat for the blood and click apply.

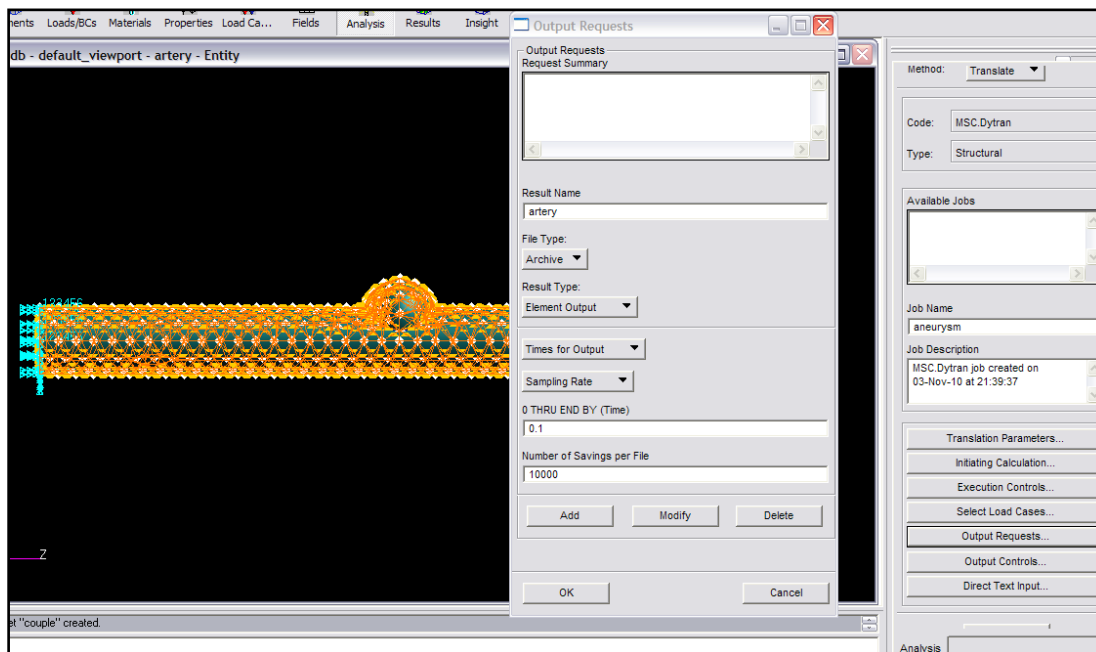


Figure 6.22: Output request

2. Analysis in MSC Dytran Software

Open MSC Dytran and select cerebral.dat as shown in Figure 6.23. Then, click start.

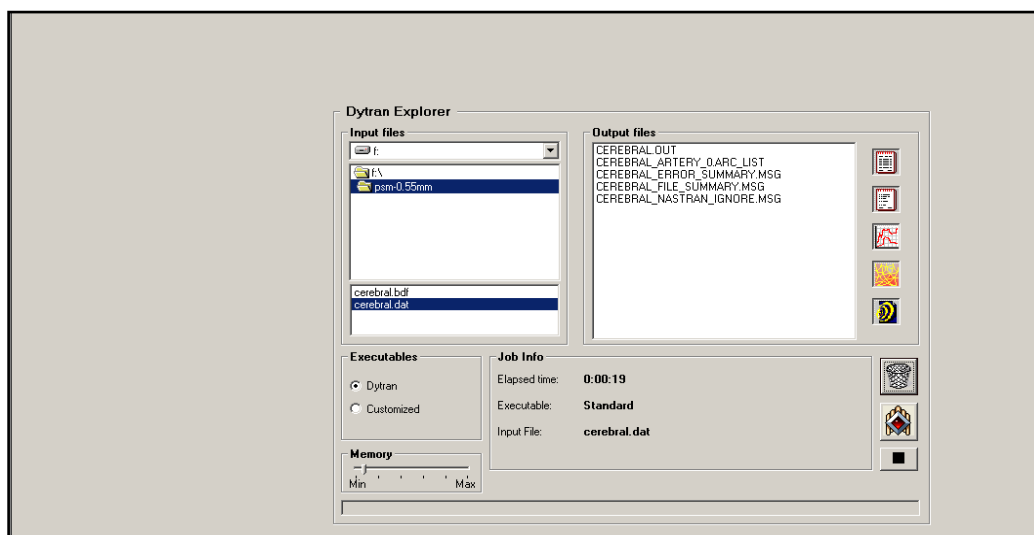


Figure 6.23: Analysis in Dytran software

3. Post-processing in MSC Patran Software

Select Analysis / read archive file / result / translate as shown in Figure 6.24. Click select archive file, select aneurysm_artery_0.ARC and click add. Select aneurysm_blood_0.ARC and click add and click apply

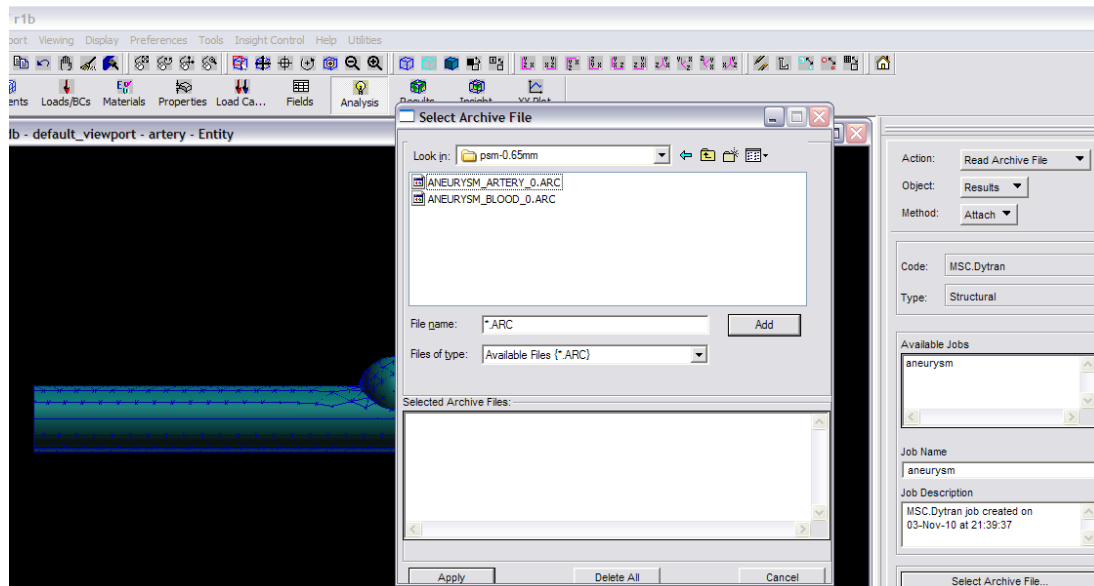


Figure 6.24: Read archive file

Select insight under preference as shown in Figure 6.25. Adjust the feature angle to 5 and clicks apply. Select Insight / create / deformation and click results selection. Select all cases, select displacement for deformation result, click animation attribute. Select cycle time for global variable and click OK. Click deformation attributes, enter 1 for scale factor, click OK and apply. Select Insight / create / isosurface. Click result selection, select all cases, select FMAT for surface result click OK and click apply. The result appeared as shown in Figure 6.26.

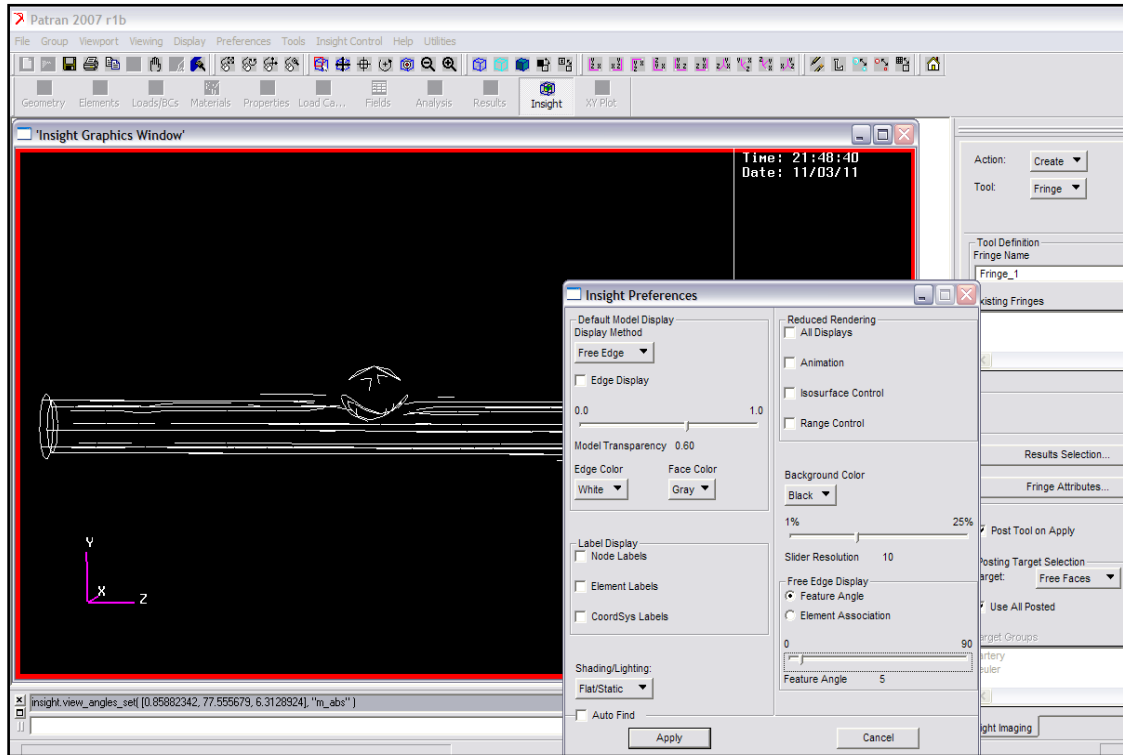


Figure 6.25: Insight

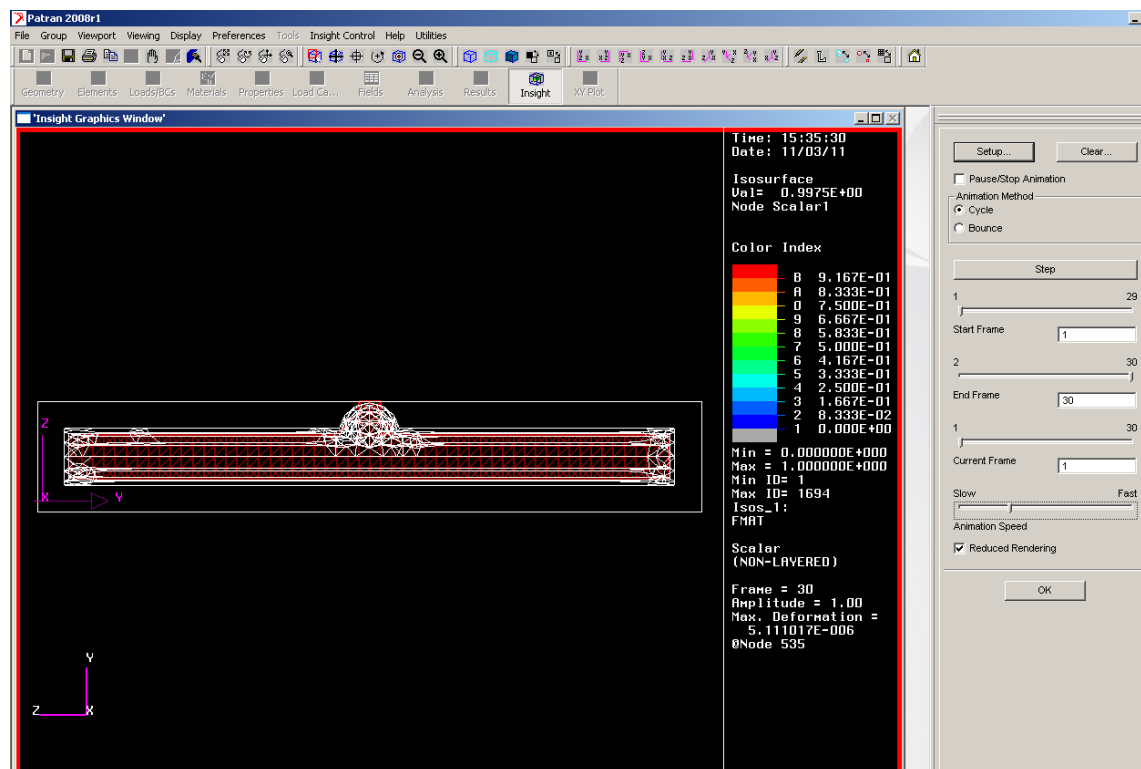



Figure 6.26: Result

APPENDIX B

APPENDIX B1: GANTT CHART

PROJECT ACTIVITIES	WEEKS													
	1	2	3	4	5	6	7	8	9	10	11	12	13	14
Identify project	Plan	Plan	Plan		Actual	Actual								
Project briefing			Plan	Plan	Plan	Plan	Actual	Actual						
Literature review				Plan	Plan	Plan	Plan	Plan	Plan					
Determine methodology										Plan	Plan	Plan	Actual	Actual
Proposal writing							Plan	Plan	Plan	Plan	Plan	Plan	Plan	Actual
Submit proposal													Actual	Actual
Presentation preparation													Actual	Actual
Present proposal													Actual	Actual

 Plan


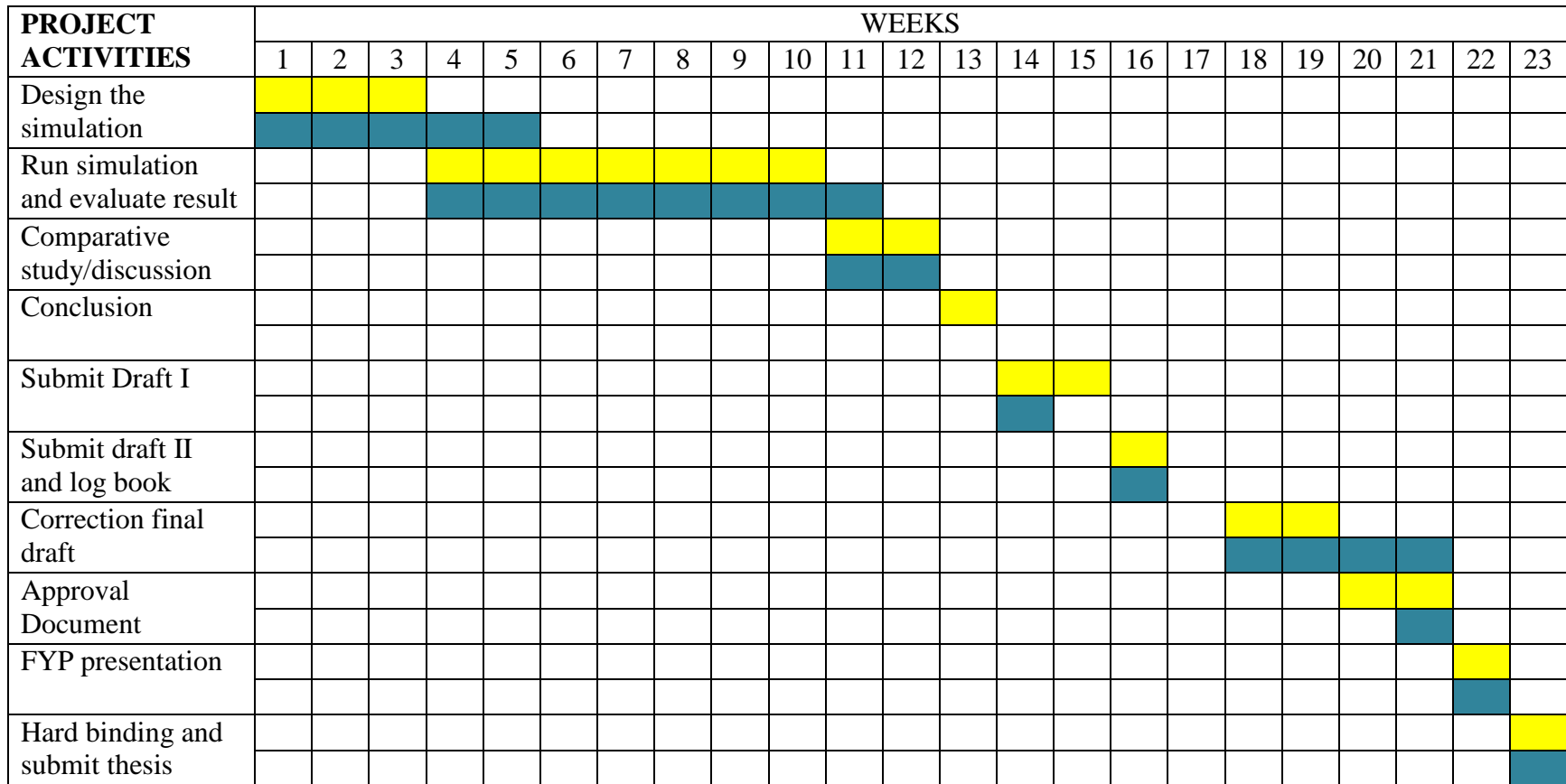

 Actual

Figure 6.27: Final Year Project (FYP) I

APPENDIX B2: GANTT CHART



 Plan


 Actual

Figure 6.28: Final Year Project (FYP) II

